Hindawi
Oxidative Medicine and Cellular Longevity
Volume 2022, Article ID 8688643, 24 pages
https://doi.org/10.1155/2022/8688643

Research Article

Melatonin Alleviates $PM_{2.5}$-Induced Hepatic Steatosis and Metabolic-Associated Fatty Liver Disease in $ApoE^{-/-}$ Mice

Zhou Du,[1,2] Shuang Liang,[1,2] Yang Li,[1,2] Jingyi Zhang,[1,2] Yang Yu,[1,2] Qing Xu,[3] Zhiwei Sun ,[1,2] and Junchao Duan [1,2]

[1]*Department of Toxicology and Sanitary Chemistry, School of Public Health, Capital Medical University, Beijing 100069, China*
[2]*Beijing Key Laboratory of Environmental Toxicology, Capital Medical University, Beijing 100069, China*
[3]*Core Facilities for Electrophysiology, Core Facilities Center, Capital Medical University, Beijing 100069, China*

Correspondence should be addressed to Zhiwei Sun; zwsun@ccmu.edu.cn and Junchao Duan; jcduan@ccmu.edu.cn

Received 6 March 2022; Accepted 6 May 2022; Published 8 June 2022

Academic Editor: Reiko Matsui

Background. Exposure to fine particulate matter ($PM_{2.5}$) is associated with the risk of developing metabolic-associated fatty liver disease (MAFLD). Melatonin is the main secreted product of the pineal gland and has been reported to prevent hepatic lipid metabolism disorders. However, it remains uncertain whether melatonin could protect against $PM_{2.5}$-induced MAFLD. *Methods and Results.* The purpose of our study was to investigate the mitigating effects of melatonin on hepatic fatty degeneration accelerated by $PM_{2.5}$ in vivo and in vitro. Histopathological analysis and ultrastructural images showed that $PM_{2.5}$ induced hepatic steatosis and lipid vacuolation in $ApoE^{-/-}$ mice, which could be effectively alleviated by melatonin administration. Increased ROS production and decreased expression of antioxidant enzymes were detected in the $PM_{2.5}$-treated group, whereas melatonin showed recovery effects after $PM_{2.5}$-induced oxidative damage in both the liver and L02 cells. Further investigation revealed that $PM_{2.5}$ induced oxidative stress to activate PTP1B, which in turn had a positive feedback regulation effect on ROS release. When a PTP1B inhibitor or melatonin was administered, SP1/SREBP-1 signalling was effectively suppressed, while Nrf2/Keap1 signalling was activated in the $PM_{2.5}$-treated groups. *Conclusion.* Our study is the first to show that melatonin alleviates the disturbance of $PM_{2.5}$-triggered hepatic steatosis and liver damage by regulating the ROS-mediated PTP1B and Nrf2 signalling pathways in $ApoE^{-/-}$ mice. These results suggest that melatonin administration might be a prospective therapy for the prevention and treatment of MAFLD associated with air pollution.

1. Introduction

Health risks associated with particulate air pollution have become a major focus of global concern due to rapid population growth, industrialization, and urbanization. Fine particulate matter at a size of $\leq 2.5\,\mu m$ ($PM_{2.5}$) has been considered as a strong potential threat to public health that it can penetrate through the alveoli of lungs into the systemic circulation and accumulate in the liver, kidney, or brain [1–3]. Recently, a precise imaging technique was developed to visualize the deposition of $PM_{2.5}$ particles in the liver through inhalation, providing solid evidence that the $PM_{2.5}$ particles can enter the extrapulmonary organs [4]. Toxicological studies have demonstrated that the toxicity of $PM_{2.5}$ not only induces respiratory and cardiovascular morbidities but also contributes to other unfavourable outcomes, such as systemic metabolic disorder, obesity, and the pathogenesis of metabolic-associated fatty liver disease (MAFLD) [2, 5], eventually resulting in liver dysfunction and damage. Consistent with evidence from animal studies, a prospective cohort study showed that people living in areas with higher $PM_{2.5}$ concentrations had a 34% higher incidence of MAFLD than those living in areas with lower $PM_{2.5}$ concentrations. The hazard ratio (HR) of MAFLD was 1.06 for every $1\,\mu g/m^3$ increase in $PM_{2.5}$ [6]. MAFLD covers a broad spectrum of liver abnormalities from hepatic steatosis to inflammation and has become one of the main cause of cirrhosis and liver cancer. Its prevalence continues to progress universally, keeping pace with the obesity epidemic, reaching 20%-30% of the total population, 80–90%

Table 1: The primer lists of real-time PCR.

Primer	Forward primer (5′-3′)	Reverse primer (5′-3′)
mus-SOD	AAGGGAGATGTTACAACTCAGG	GCTCAGGTTTGTCCAGAAAATG
hsa-SOD	CCCGACCTGCCCTACGACTAC	AACGCCTCCTGGTACTTCTCCTC
mus-Keap1	GACTGGGTCAAATACGACTGC	GAATATCTGCACCAGGTAGTCC
hsa-Keap1	ATTCAGCTGAGTGTTACTACCC	CAGCATAGATACAGTTGTGCAG
mus-Nrf2	CAGCCATGACTGATTTAAGCAG	CAGCTGCTTGTTTTCGGTATTA
hsa-Nrf2	TCCAAGTCCAGAAGCCAAACTGAC	GGAGAGGATGCTGCTGAAGGAATC
mus-SREBP1	GCTACCGGTCTTCTATCAATGA	CGCAAGACAGCAGATTTATTCA
hsa-SREBP1	CTGTGTGACCTGCTTCTTGT	CTCATGTAGGAACACCCTCC
mus-SP1	GAAGCAGCAGCACAGGCAGTAG	GCCAGCAGAGCCAAAGGAGATG
hsa-SP1	TCACTCCATGGATGAAATGACA	CAGAGGAGGAAGAGATGATCTG
mus-PP2A	AGTTACACTGCTTGTAGCTCTT	AACCCATAAACCTGTGTGATCT
hsa-PP2A	CGAAGGTGTGAAGGGGAAGAAGC	CAGCGTGTTGAGAAGAGCGACTAG
mus-PTP1B	GAGAGATCCTGCATTTCCACTA	TACTTTCTTGATGTCCACGGAA
hsa-PTP1B	CCATTTACCAGGATATCCGACA	TGACGTCTCTGTACCTATTTCG

of obese individuals, and even more subjects with type 2 diabetes mellitus (T2DM) [7].

The mechanism for the pathophysiology of MAFLD was initially explained by the "two-hit" hypothesis. The first hit is that insulin resistance leads to enhanced hepatic de novo lipogenesis and decreased lipolysis. Mice exposed to $PM_{2.5}$ have been demonstrated to develop MAFLD, characterized by changes in liver appearance, extensive distribution of lipid vacuoles, and balloon-like degeneration within the lobular structure [5, 8]. The accumulation of free fatty acid flux in hepatic cells further triggers a "second hit" involving oxidative stress and lipid peroxidation [9]. It has also been reported that $PM_{2.5}$ exposure induces excessive oxygen species (ROS) production and redox homeostasis disorder [10, 11]. In brief, oxidative stress appears to be an integral mechanism that conveys hepatic injury in MAFLD and plays a well-described role in mediating the toxicity of $PM_{2.5}$ [12]. However, the specific mechanism by which $PM_{2.5}$ exposure promotes the risk of oxidative stress-driven MAFLD remains incompletely understood.

A growing body of evidence in the cellular and molecular biology of lipid metabolism have shown that protein tyrosine phosphatase 1B (PTP1B) is a new activator in the process of MAFLD that regulates lipogenesis in the liver [13, 14]. Total PTP1B protein levels were generally upregulated in liver biopsies from patients with MAFLD [15]. Functionally, PTP1B deficiency prevents the adverse metabolic effects of a high-fat diet, including weight gain, increased liver lipids, and reduced glucose tolerance [16]. $PTP1B^{-/-}$ mice also exhibited downregulation of genes involved in fat production, including sterol regulatory element-binding proteins (SREBPs) [17]. Furthermore, SREBP-1 could extensively affect multiple metabolic steps in the liver and extranet, thereby regulating the progression of MAFLD [18]. However, it is still not clear whether $PM_{2.5}$ has a targeted regulatory effect on PTP1B.

Melatonin is well-known for its ability to neutralize ROS and reduce oxidative stress [19]. It upregulates nuclear factor erythroid 2-related factor 2 (Nrf2) through inhibition of Kelch—like ECH-associated protein (Keap1) to suppress oxidative stress in the liver [20]. Investigations have noted that melatonin critically participates in lipid metabolism and potentially contributes to the onset and progression of MAFLD [21, 22]. However, it remains uncertain whether melatonin could protect against $PM_{2.5}$-induced oxidative stress in the liver and ameliorate MAFLD.

Compared with the general population, people with obesity, hyperlipidaemia, or abnormal lipid metabolism are more sensitive to $PM_{2.5}$ and have a higher risk of developing MAFLD [23, 24]. According to a cohort study of full-exome association of alanine aminotransferase, ApoE was found closely linked with fatty liver [25], and allele-specific variants of ApoE were associated with an increased incidence of MAFLD and obesity [26]. Thus, intense efforts have been made to investigate MAFLD based on $ApoE^{-/-}$ mice [27–30]. Hua et al. demonstrated that naringin administration improved metabolic parameters in $ApoE^{-/-}$ mice, inhibited hepatic steatosis, and reduced hepatic fibrosis [31]. Stachowicz et al. found that high fat diet resulted in more exacerbated hepatic steatosis in $ApoE^{-/-}$ mice [32]. In this study, $ApoE^{-/-}$ mice were chosen as an animal model to explore the molecular mechanism of the melatonin-mediated protective effects against $PM_{2.5}$-induced MAFLD. We speculated that melatonin may ameliorate $PM_{2.5}$-induced MAFLD. Our findings supported this hypothesis and further indicated that melatonin alleviated the disturbance of $PM_{2.5}$-triggered hepatic steatosis and liver damage by regulating the ROS-mediated PTP1B and Nrf2 signalling pathways. These results not only provide novel insight into the underlying molecular mechanism by which $PM_{2.5}$ contributes to the pathogenesis of MAFLD but also suggest the use of melatonin as a potential treatment.

2. Materials and Methods

2.1. Collection and Extraction of $PM_{2.5}$. $PM_{2.5}$ was collected on quartz fibre filters with a special sampler (TH-1000C, Wuhan Tianhong, China) from Capital Medical University

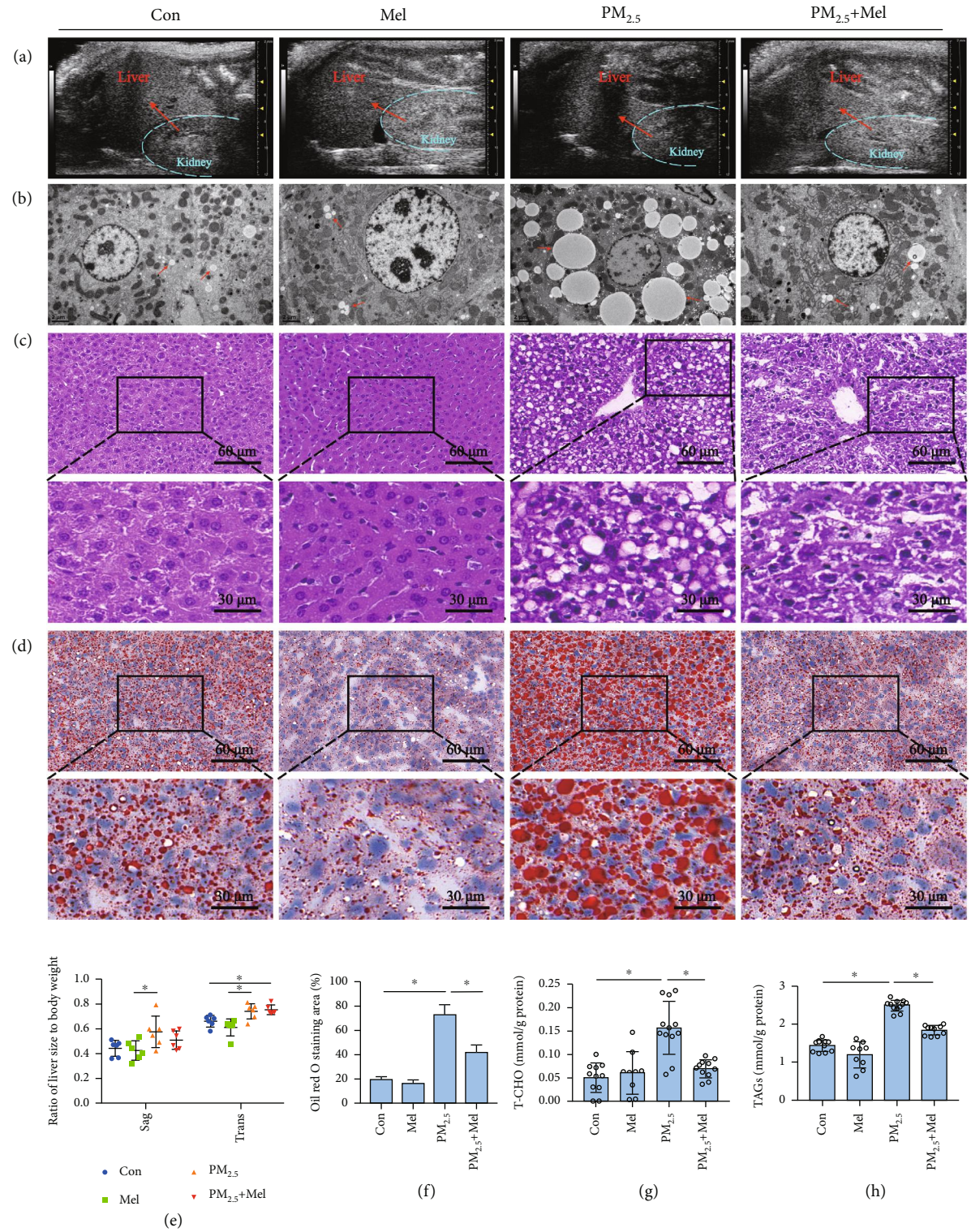

Figure 1: Melatonin improved the increased lipid content and steatosis in the liver induced by $PM_{2.5}$. (a) Ultrasound examination of liver—comparison of liver echo and kidney echo. (b) The ultrastructure of liver tissues via electron microscopy (magnification, 200; scale bar, 2 μm). (c) Liver sections with haematoxylin and eosin (H&E) staining (magnification, 200 and 400; scale bar, 60 μm and 30 μm). (d) Liver steatosis assessed by Oil Red O staining (magnification, 200 and 400; scale bar, 60 μm and 30 μm). (e) Liver sag (anterior-posterior diameter) and liver trans (left-right diameter) measurement to mice weight ratio. (f) The ratio of the Oil Red O-stained area to the total tissue area. (g) Hepatic total cholesterol lipid levels (mmol/g). (h) Hepatic triacylglycerol lipid levels (mmol/g). Con: animals were treated with saline; Mel: animals were treated with melatonin; $PM_{2.5}$: animals were treated with $PM_{2.5}$; $PM_{2.5}$+Mel: animals were treated with melatonin and $PM_{2.5}$. Data are shown as means ± SD. $n = 6 - 12$ mice per group. $^*P < 0.05$ for Con group vs $PM_{2.5}$ group and $PM_{2.5}$ group vs $PM_{2.5}$+Mel group.

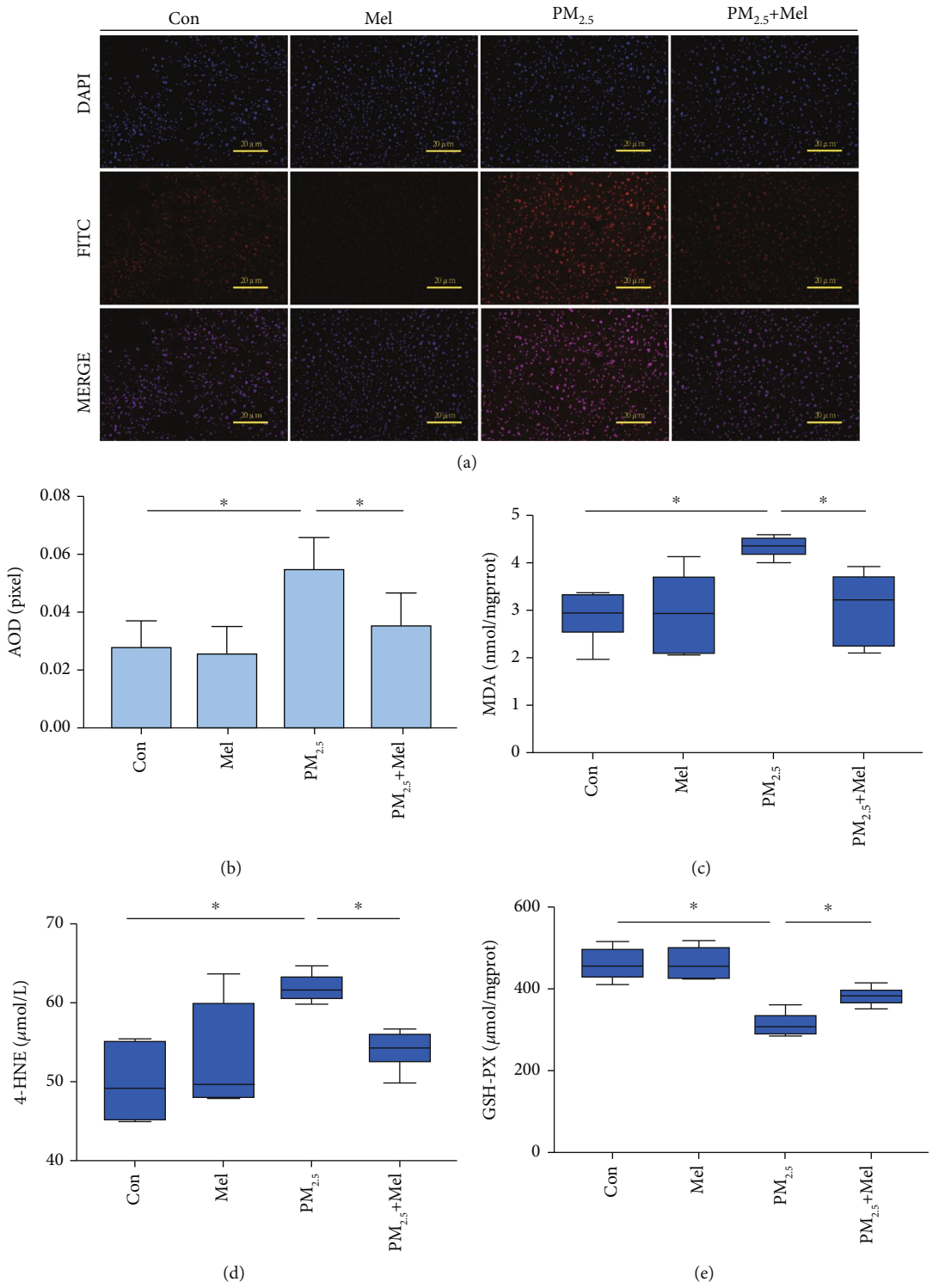

Figure 2: Continued.

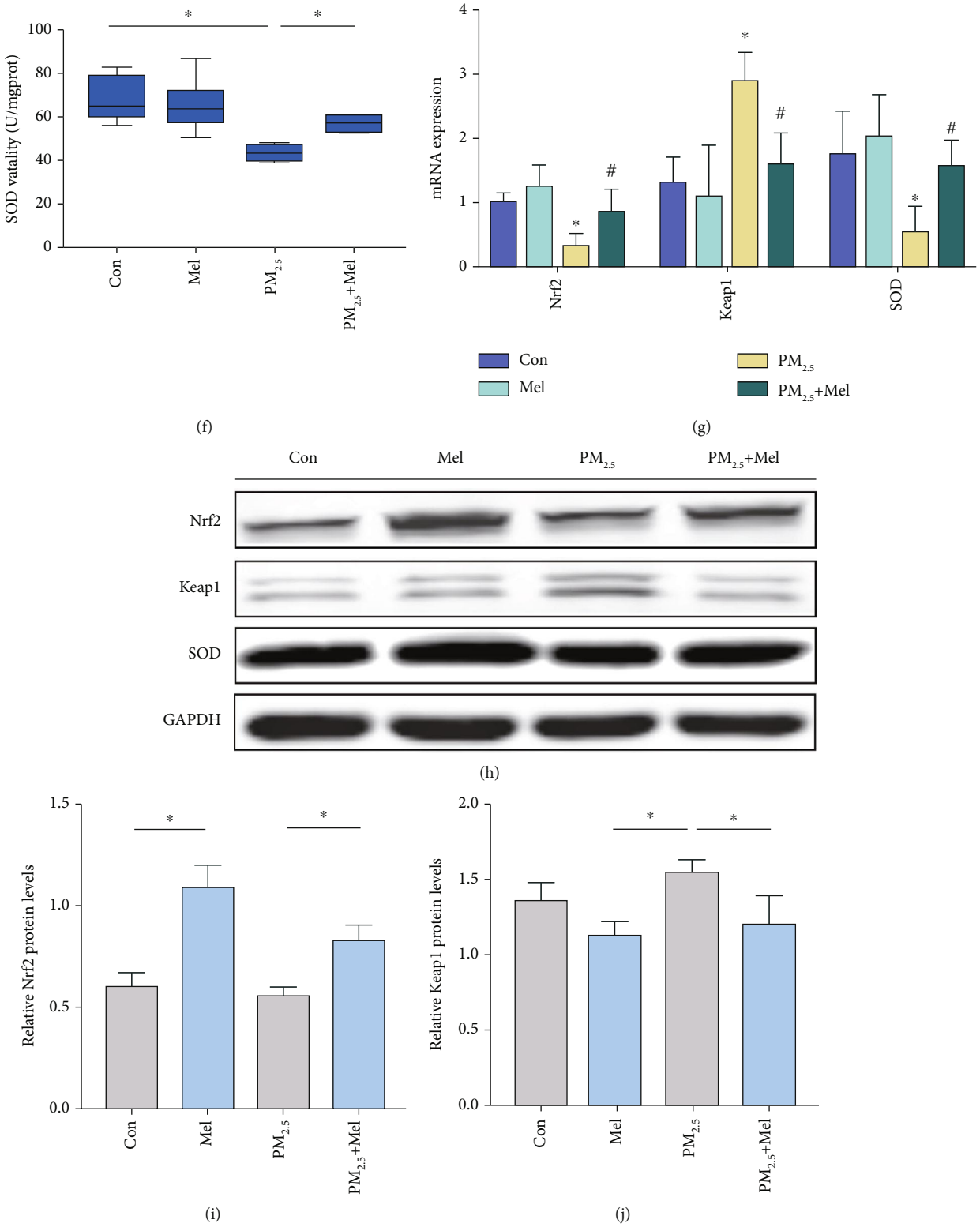

Figure 2: Continued.

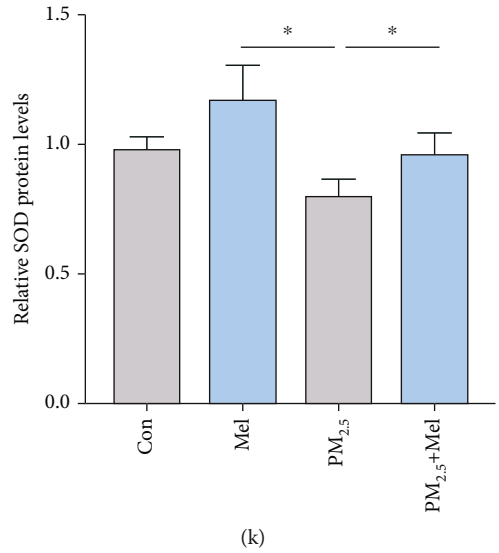

Figure 2: Melatonin improved liver oxidative damage induced by $PM_{2.5}$. (a) Production of ROS detected by the fluorescent probe DHE (magnification, 200; scale bar, 20 μm). (b) Quantitative analysis of ROS production is reflected by the mean fluorescence intensity as shown in different groups. (c) The level of MDA. (d) The level of 4-HNE. (e) The level of GSH-PX. (f) The vitality of SOD. (g) The mRNA expression of Nrf2, Keap1, and SOD. (h) Western blotting of Nrf2, Keap-1, and SOD. (i) Protein quantification of Nrf2. (j) Protein quantification of Keap1. (k) Protein quantification of SOD. All values are presented as the mean ± SD ($n = 6$). $^{*}P < 0.05$ for Con group vs $PM_{2.5}$ group and $^{\#}P < 0.05$ for $PM_{2.5}$ group vs $PM_{2.5}$+Mel group.

(Beijing, China) for the entire year of 2017. The physicochemical characterization of $PM_{2.5}$ was described in detail in our previous study. Tables S1 and S2 show the results of element analysis. S, Ca, Na, Si, and Fe are the most abundant elements. Toxic heavy metals (including Mn, Cd, Cr, Ni, and Sb), toxic nonmetallic elements (As), and water-soluble ions (NO_3^-, $SO4_2^-$, and $NH4^+$) were detected in $PM_{2.5}$ [33, 34]. Sampled filters were placed in ultrapure water for 3 hours using an ice-water bath ultrasonic instrument. Then, freeze-dried samples were irradiated with ultraviolet light for 2 hours, diluted and mixed with pure water, and suspended in $PM_{2.5}$ by ultrasonication for 30 minutes for later use.

2.2. Animals and Treatments. Seven-week-old male $ApoE^{-/-}$ mice (specific-pathogen free) were obtained from the Experimental Laboratory Animal Technology Co., Ltd. (Vital River, Beijing, China). Animal experimental procedures were approved by the Experimental Animal Welfare Committee (Capital Medical University; AEEI-2016-076). All mice were fed a high-fat diet (0.15% cholesterol and 21% fat). After acclimatization for one week, a total of 60 mice were randomly divided into four groups: (i) control group (Con): animals were treated with saline; (ii) $PM_{2.5}$ group ($PM_{2.5}$): animals were treated with $PM_{2.5}$; (iii) melatonin group (Mel): animals were treated with melatonin; and (iv) melatonin and $PM_{2.5}$ group ($PM_{2.5}$+Mel): animals were treated with $PM_{2.5}$ and melatonin. Mice were orally gavaged with melatonin (20 mg/kg•bw, in 20~25 μL of 0.5% ethanol solution) daily and $PM_{2.5}$ (5 mg/kg•bw, in 20~25 μL of saline) via intratracheal instillation twice a week for 4 weeks. The control mice received a corresponding volume of blank filters eluted with saline by intratracheal instillation. The vehicle mice were gavaged with the same amount of sterile water (0.5% ethanol).

According to the concentration and intervention method of melatonin in previous studies, melatonin (Sigma, USA) was dissolved in absolute ethanol and diluted in sterile water to a final concentration of 0.5% ethanol, with the oral gavage at a dose of 20 mg/kg/day [35, 36]. The dose of $PM_{2.5}$ exposure was based on the respiratory physiological parameters of mice and the annual mean $PM_{2.5}$ concentration (35 $\mu g/m^3$), according to the WHO air quality guidelines [37]. The respiratory volume of an adult mouse (25 g) is 0.15 mL at each breath, and the breath rate is 163 times per min, and respiratory volume for one day reaches 0.035208 m^3. For this reason, the daily exposure of mice was $0.035208 * 35\ \mu g/m^3 = 1.23228\ \mu g$. Based on the body weight of mice 25 g and the extrapolation coefficient of species 100, the volume of intratracheal instillation was $1.23228\ \mu g/25\ g * 100 = 4.93\ \mu g/g$. Previous studies have demonstrated that $PM_{2.5}$ at 5 mg/kg can cause varying degrees of organ damage [38, 39]. Therefore, a dose of 5 mg/kg was selected for animal modeling.

2.3. Ultrasonic Examination of Liver. Before ultrasound imaging, the mice were fasted for 12 h, the abdominal regions were shaved, and then the mice were anaesthetized with a saturated tribromoethanol solution via intraperitoneal injection. We acquired transcutaneous ultrasound images using a Vevo2100 Ultrasonic Doppler System (Fujifilm Visual Sonics, US).

2.4. Histopathological Examination. Both haematoxylin-eosin (H&E) and Oil Red O staining are effective and reproducible methods for quantifying hepatic steatosis [40]. For

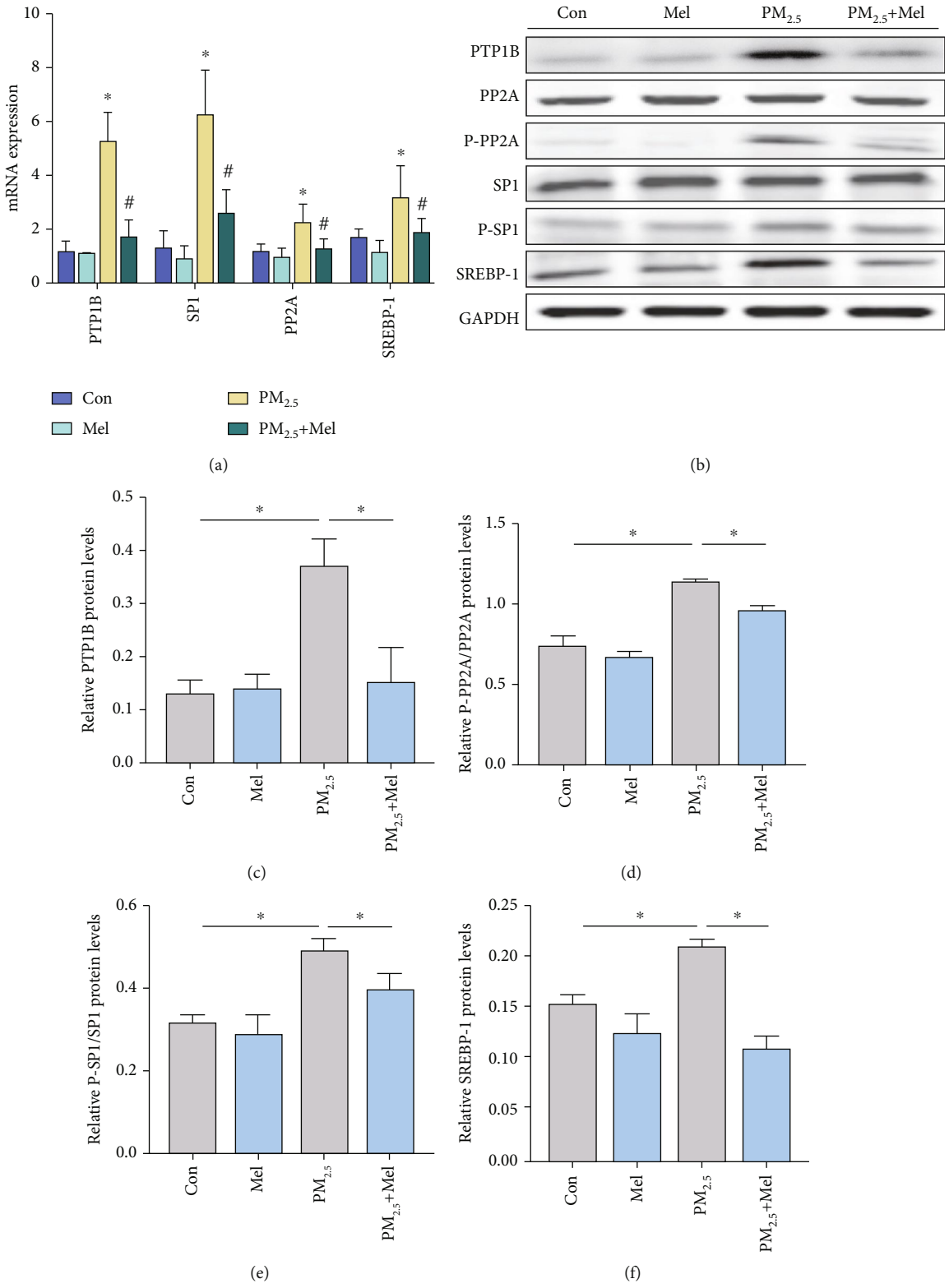

Figure 3: Continued.

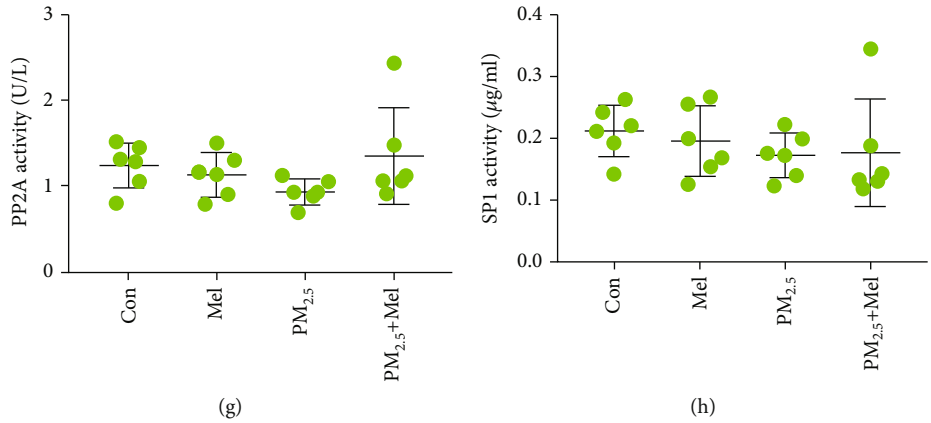

FIGURE 3: Melatonin ameliorated abnormal liver lipid metabolism caused by elevated PTP1B expression induced by $PM_{2.5}$. (a) The mRNA expression of PTP1B, PP2A, SP1, and SREBP-1. (b) Western blotting of PTP1B, PP2A, P-PP2A, SP1, P-SP1, and SREBP-1. (c) Protein quantification of PTP1B. (d) Protein quantification of P-PP2A/PP2A. (e) Protein quantification of P-SP1/SP1. (f) Protein quantification of SREBP-1. (g) The activity of PP2A. (h) The activity of SP1. All values are presented as the mean ± SD ($n = 6$). $^{*}P < 0.05$ for Con group vs $PM_{2.5}$ group and $^{\#}P < 0.05$ for $PM_{2.5}$ group vs $PM_{2.5}$+Mel group.

histological examination, liver specimens were fixed overnight with 4% paraformaldehyde and then embedded in paraffin sections (4–6 μm). Tissue sections were counterstained with H&E. To visualize lipid droplet accumulation, frozen liver sections (10 μm) were taken, stained with Oil Red O (0.5%) for 10 min, washed and rinsed with isopropanol, and counterstained with haematoxylin for a few seconds. Representative photographs were taken at 200x and 400x magnification using an in-microscope system. There were 6 samples in each group, and twenty regions were randomly selected from each separate section. The "color picker" in Image-Pro-Plus was used to select the red fat droplets in images until all the red fat droplets were marked. Then, Oil Red O-stained area was measured, and its ratio to the total tissue area was calculated.

2.5. Ultrastructural Observation by Transmission Electron Microscopy (TEM). Lipid accumulation in the liver tissue was observed by transmission electron microscopy. The liver tissues were immediately placed into 2.5% glutaraldehyde for 10 min at 4°C and then washed with PBS 3 times and dehydrated. Sample sections (60 nm) were stained on copper mesh and assessed using TEM (JEM-2100plus).

2.6. Detection of ROS Levels in Liver Tissue. Frozen sections of the liver were washed, DHE solution (10 μM) was added, and the sections were incubated at room temperature for 30 min. A confocal microscope (LSCM, TCS SP8 STED, Germany) was used to capture fluorescence images. There were 6 samples in each group, and 3 visual fields were randomly selected for each sample. Then, the ratio of red area to total area was statistically analyzed by Image-Pro-Plus.

2.7. Cell Culture and Treatment. The human normal liver cell line L02 was obtained from Shanghai Institutes for Biological Sciences (SIBS, China). Cells were cultured in Dulbecco's modified Eagle's medium (DMEM; Corning, USA) containing 1% penicillin-streptomycin solution and 10% foetal bovine serum (Corning, USA) at 37°C in a humidified incubator with 5% CO_2. Palmitic acid (PA) is an inducer for cell steatosis. For treatment before each experiment, cells were treated with PA solution dissolved in DMEM for 24 h. When the cell density reached 70%-80%, DMEM (without serum) containing $PM_{2.5}$ or melatonin was added and then cultured for 24 h. The control group was cultured in a constant volume of pure medium.

2.8. Assessment of Cytotoxicity. A total of 1×10^4 L02 cells per well were seeded in 96-well culture plates. When the cell density reached 50%, the L02 cells were exposed to gradient concentrations of $PM_{2.5}$ (0, 12.5, 25, and 50 100 μg/mL), PA (0, 50, 100, 200, 400, 800, and 1600 μmol/L), and melatonin (0, 12.5, 25, 50, 100, and 200 μmol/L). According to the protocols, cell viabilities were measured by Cell Counting Kit-8 (CCK-8, Tongren, Japan), and the absorbance was measured at 450 nm using a microplate reader (Thermo, USA).

2.9. Biochemical Parameter Analysis. Triacylglycerols (TAGs), total cholesterol (TC), low-density cholesterol (LDL-C), high-density cholesterol (HDL-C), glutathione peroxidase (GSH-Px), superoxide dismutase (SOD), and malonaldehyde (MDA) levels were measured spectrophotometrically according to the instructions of the kit (Nanjing Jiancheng Institute of Biotechnology, Nanjing, China). Protein concentration was determined using a BCA protein assay kit (Dingguo Changsheng Biotech, China). The 4-hydroxynonenal (4-HNE) activity was determined using a Hailian Biotechnology Co. Ltd. ELISA (enzyme-linked immunosorbent assay) kit (Jiangxi, China).

2.10. Cellular BODIPY Staining. BODIPY™ 493/503 (Thermo, USA) is a lipophilic fluorescent probe targeting polar lipids that can be used to label cell neutral lipid content, especially lipid content localized to lipid droplets. It was dissolved in anhydrous ethanol to generate a 10 mM stock solution, which was frozen, dried, and stored away

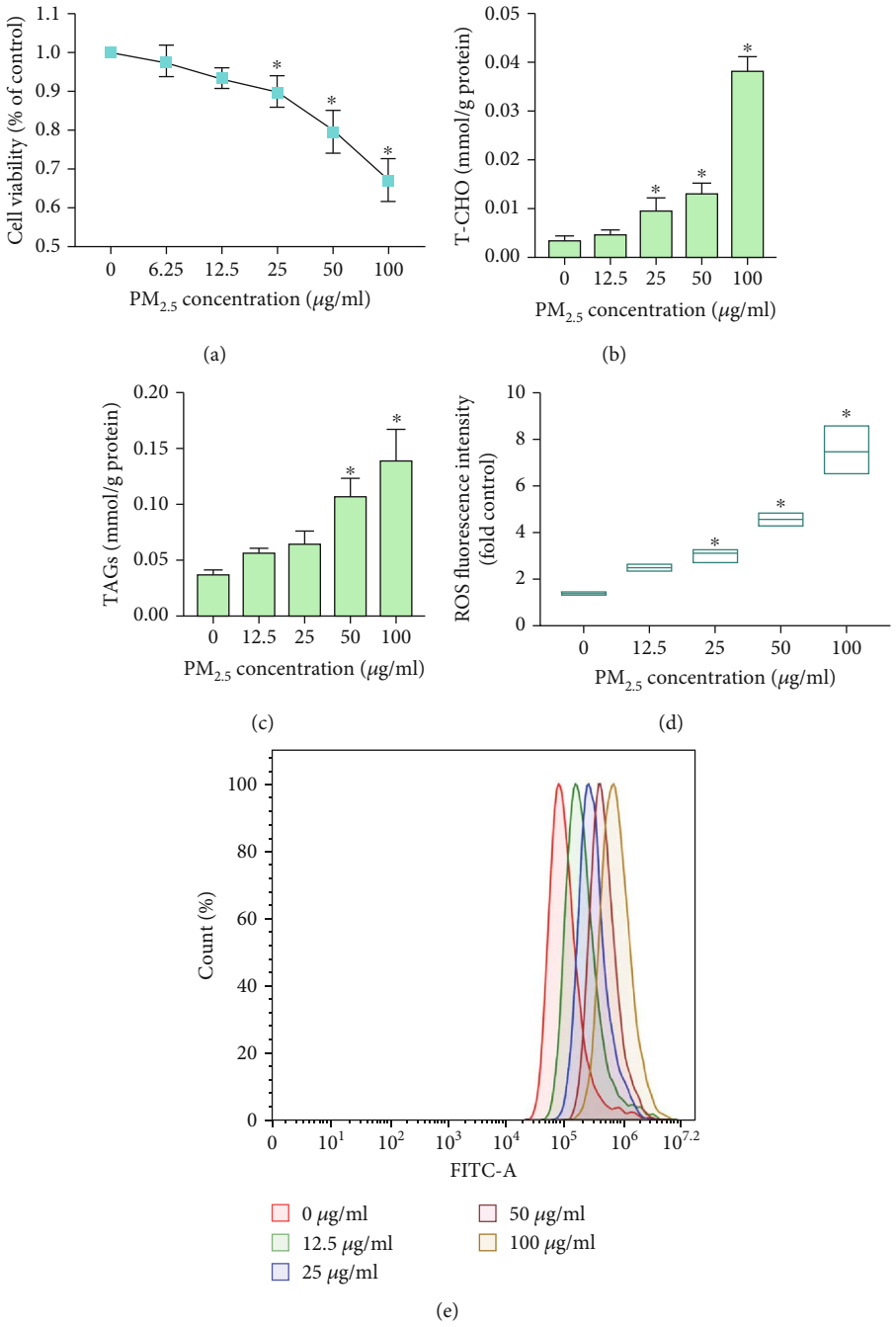

Figure 4: Continued.

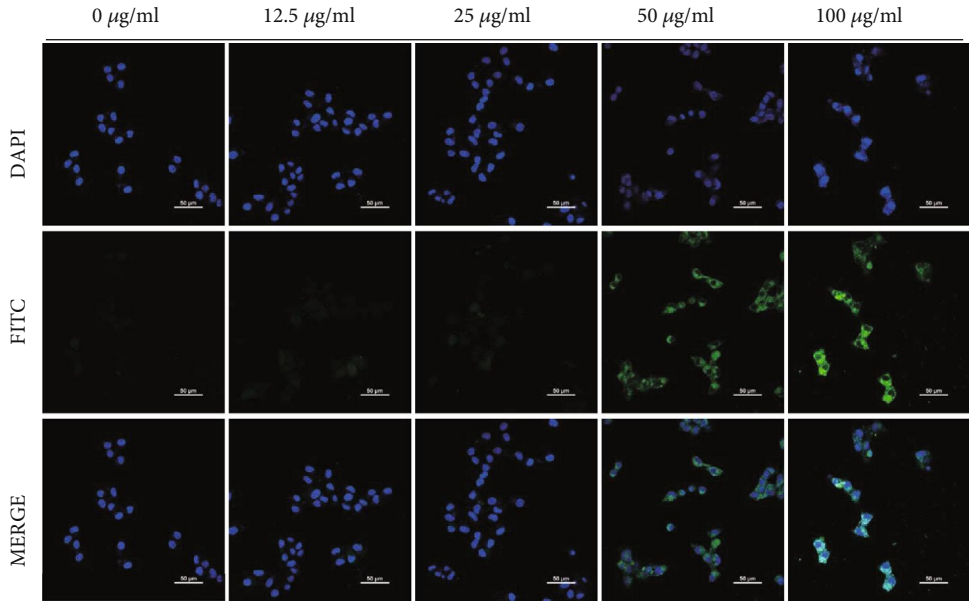

(f)

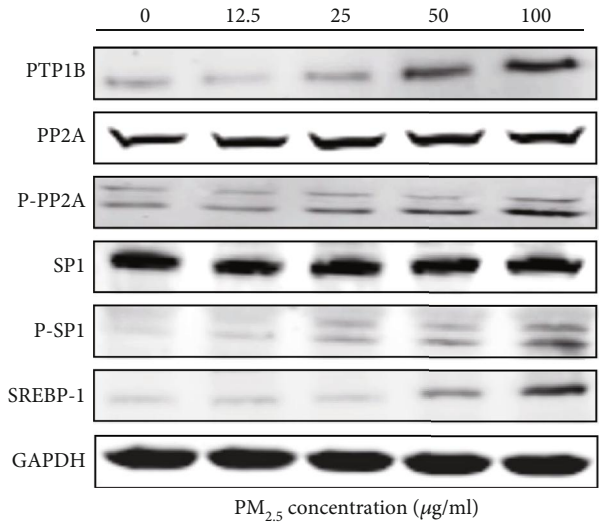

(g)

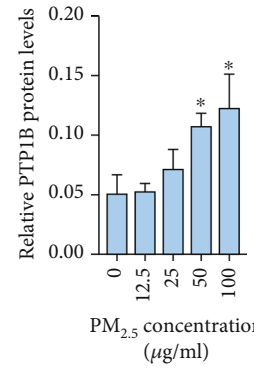

(h)

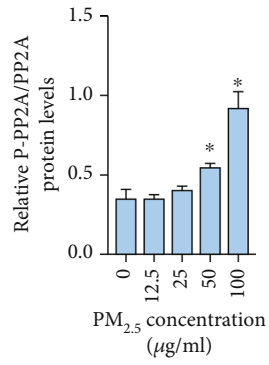

(i)

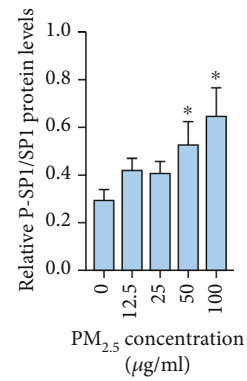

(j)

Figure 4: Continued.

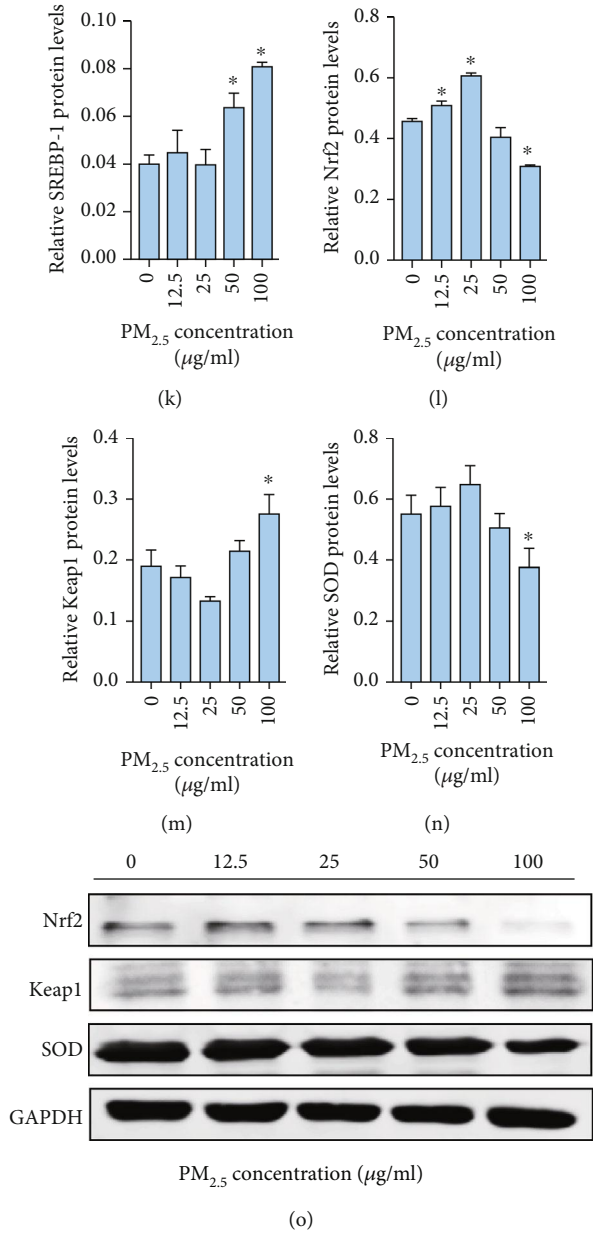

FIGURE 4: $PM_{2.5}$ induced lipid accumulation in hepatocytes. (a) Cell viability. (b) Total cholesterol lipid levels (mmol/g). (c) Triacylglycerol lipid levels (mmol/g). (d) Representative fluorescence intensity images obtained from flow cytometry in L02 cells. (e) Analysis of fluorescence intensity obtained from flow cytometry. (f) Representative confocal images of ROS. (g) Western blotting of PTP1B, PP2A, P-PP2A, SP1, P-SP1, and SREBP-1. (h) Protein quantification of PTP1B. (i) Protein quantification of P-PP2A/PP2A. (j) Protein quantification of P-SP1/SP1. (k) Protein quantification of SREBP-1. (l) Protein quantification of Nrf2. (m) Protein quantification of Keap1. (n) Protein quantification of SOD. (o) Western blotting of Nrf2, Keap1, and SOD. All values are presented as the mean ± SD. $^*P < 0.05$.

from light. PBS was used to dilute the solution to 10 μM, which was used for incubation with the cells at room temperature in the dark for 20 min; finally, the cells were observed via a confocal microscope (LSCM, TCS SP8 STED, Germany).

2.11. Detection of ROS Levels in L02 Cells. The level of ROS in L02 cells was analyzed by flow cytometry. After the cells were infected for 24 h, a 2′,7′-dichlorofluorescein diacetate (DCFH-DA, Sigma, USA) working solution (10 μM) was added followed by incubation at 37°C for 30 min. The cells were washed twice with PBS, and ROS levels were determined by flow cytometry. The single-parameter histograms were obtained by taking the logarithm of fluorescence signal as abscissa and the number of cells as ordinate, which could intuitively reflect the relative intensity of ROS in living cells. The average fluorescence intensity was the number of cells divided by the area under each peak. ROS fluorescence was measured with a confocal scanning laser microscope. To quantify the ROS production in L02 cells treated with

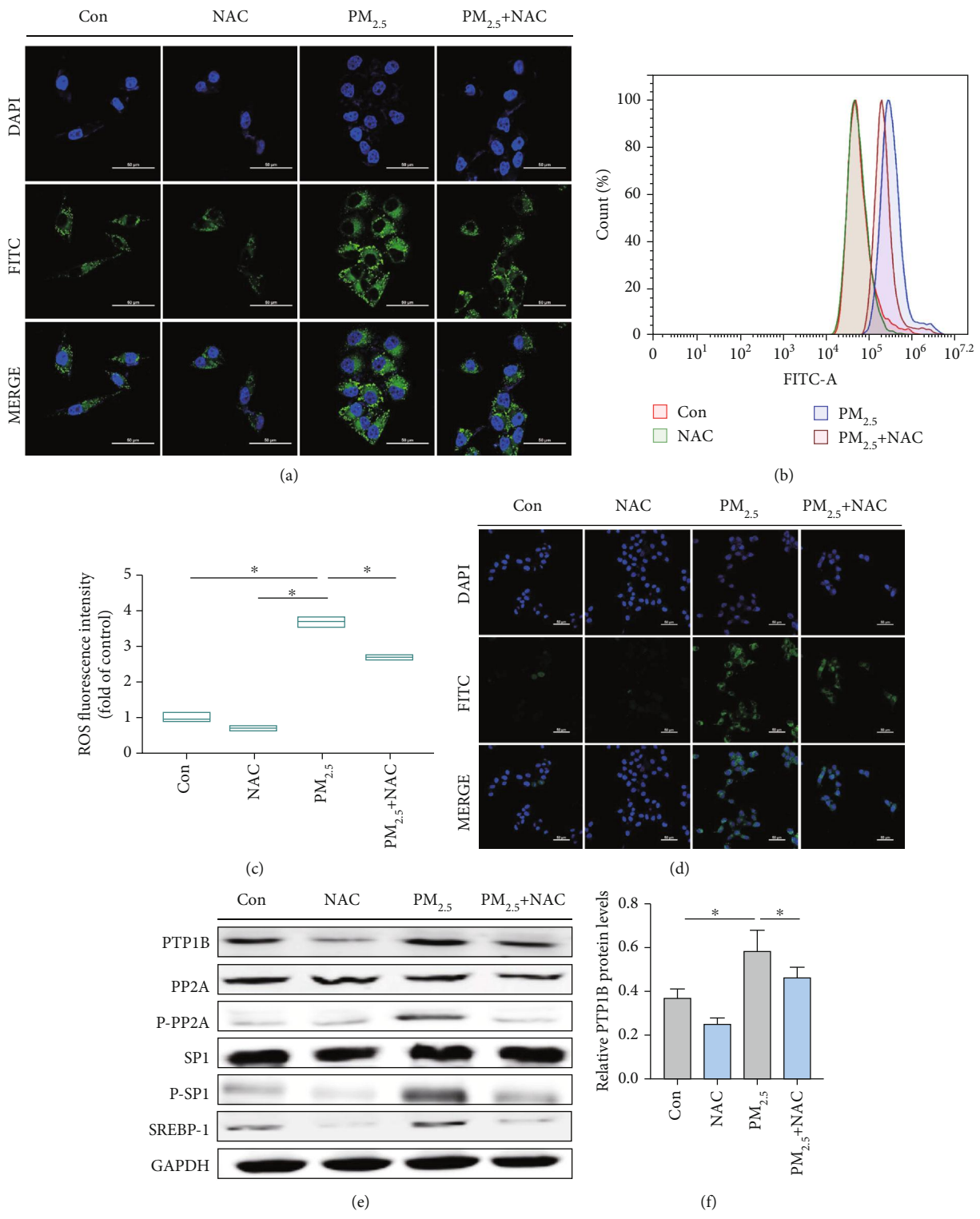

Figure 5: Continued.

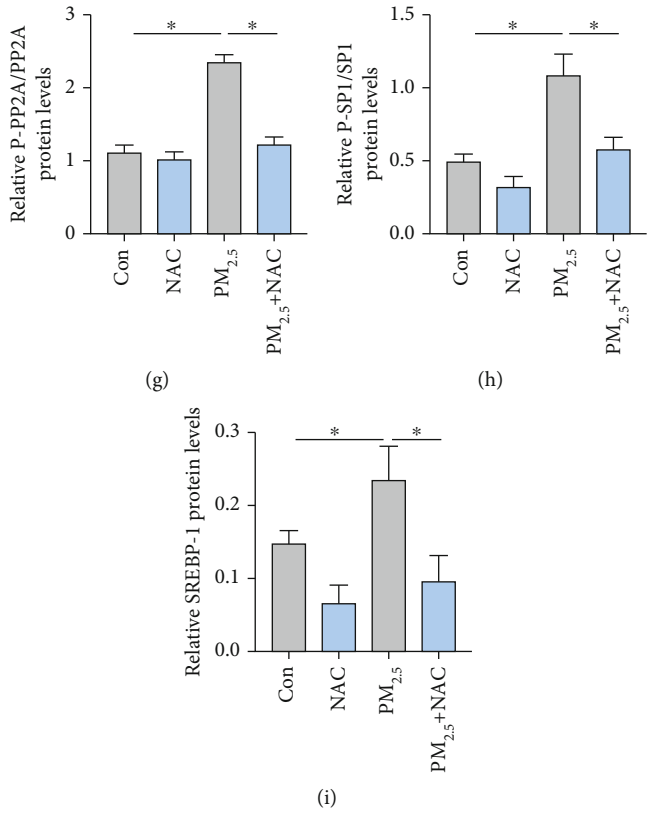

FIGURE 5: $PM_{2.5}$ induced lipid accumulation in hepatocytes by increasing ROS levels and PTP1B expression. (a) BODIPY staining of L02 cells (scale bar, 50 μm). (b) Representative fluorescence intensity images obtained from flow cytometry in L02 cells. (c) Analysis of fluorescence intensity obtained from flow cytometry. (d) Representative confocal images of ROS. (e) Western blotting of PTP1B, PP2A, P-PP2A, SP1, P-SP1, and SREBP-1. (f) Protein quantification of PTP1B. (g) Protein quantification of P-PP2A/PP2A. (h) Protein quantification of P-SP1/SP1. (i) Protein quantification of SREBP-1. All values are presented as the mean ± SD. $^*P < 0.05$.

$PM_{2.5}$ and/or melatonin, cells were pretreated with the ROS inhibitor N-acetylcysteine (NAC; Sigma, USA) (1 mM) for 1 h before $PM_{2.5}$ and/or melatonin exposure.

DCFH-DA, intracellular reactive oxygen species detection probe, is a universal indicator of oxidative stress. After it enters the cell, it is hydrolyzed to produce DCFH. Intracellular reactive oxygen species can oxidize nonfluorescent DCFH to produce fluorescent DCF. Intracellular reactive oxygen species (ROS) levels were obtained by measuring the fluorescence intensity of DCF.

2.12. Real-Time Polymerase Chain Reaction (qPCR). Total RNA from L02 cells and liver tissue was extracted using TRIzol™ Reagent (Thermo, USA). According to the protocol, the RNA was reverse transcribed into cDNA with PrimeScript RT Master Mix (Takara, China). SYBR® Premix Ex Taq™ II (Takara, China) was used for quantitative PCR on a Realplex2 (Eppendorf, Germany). The mRNA primers are listed in Table 1.

2.13. Western Blot Analysis. Protein extracts of mouse liver tissue and L02 cells were prepared by a Whole Cell Lysis Assay Kit (Keygen Biotech, China), and the concentrations were determined by a BCA protein quantitative assay kit (Dingguo Changsheng Biotech, China). The same amounts of protein were separated by electrophoresis using 8%–12% SDS-PAGE gels and transferred to suitably sized nitrocellulose membranes (Pall Corp., USA). After blocking with 5% BSA or 5% skim milk in Tris-buffered saline (TBS), the membranes were incubated with primary antibodies at 4°C overnight, including PTP1B (Abcam, UK), SP1 (Abcam, UK), P-SP1 (Abcam, UK), SOD (Abcam, UK), Nrf2 (Abcam, UK), Keap1 (Abcam, UK), PP2A (Santa, USA), P-PP2A (Santa, USA), SREBP-1 (Santa, USA), and GAPDH (CST, USA). The next day, the membranes were washed three times with TBST and incubated with an anti-rabbit/mouse IgG secondary antibody (CST, USA). A LI-COR Odyssey system (LI-COR Biosciences, USA) was used for detection of the protein bands, which were quantified using Image Studio software (NIH, Bethesda, MD).

2.14. The Addition of PTP1B Inhibitor. We dissolve PTP1B inhibitor PTP1B-IN-1 (MedChemExpress, USA) in DMSO to prepare a stock solution at a concentration of 20 mM. Then, L02 cells were treated with PTP1B-IN-1 (5 μg/mL, 10 μg/mL, 20 μg/mL, and 40 μg/mL) diluted with DMEM for 12 h. After qPCR analysis, 10 μg/mL was selected as the dose of PTP1B-IN-1.

2.15. Statistical Analysis. SPSS 24.0 software was used to analyze all experimental data. Data are presented as the mean ± SD. Data consistent with a normal distribution and an

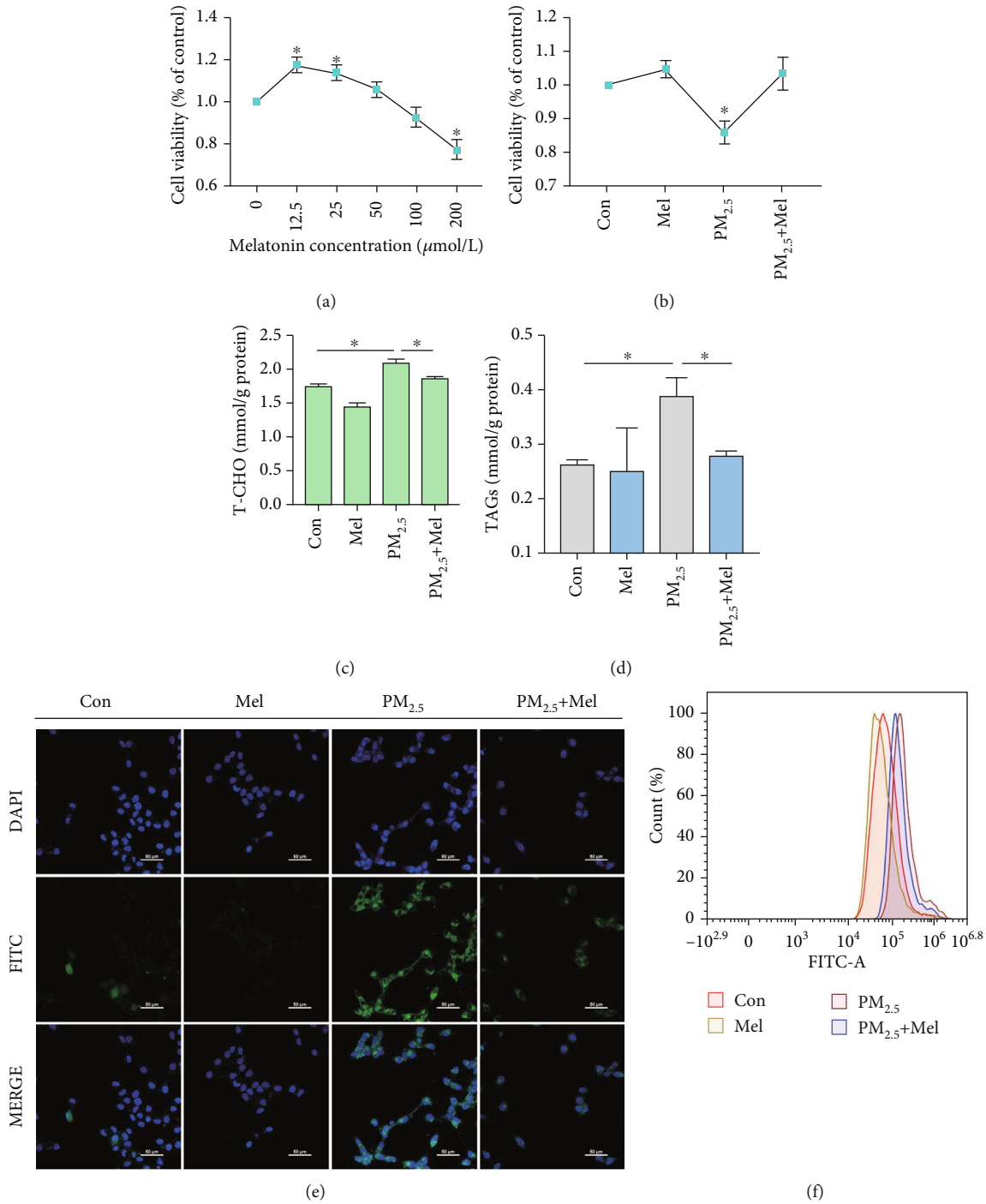

Figure 6: Continued.

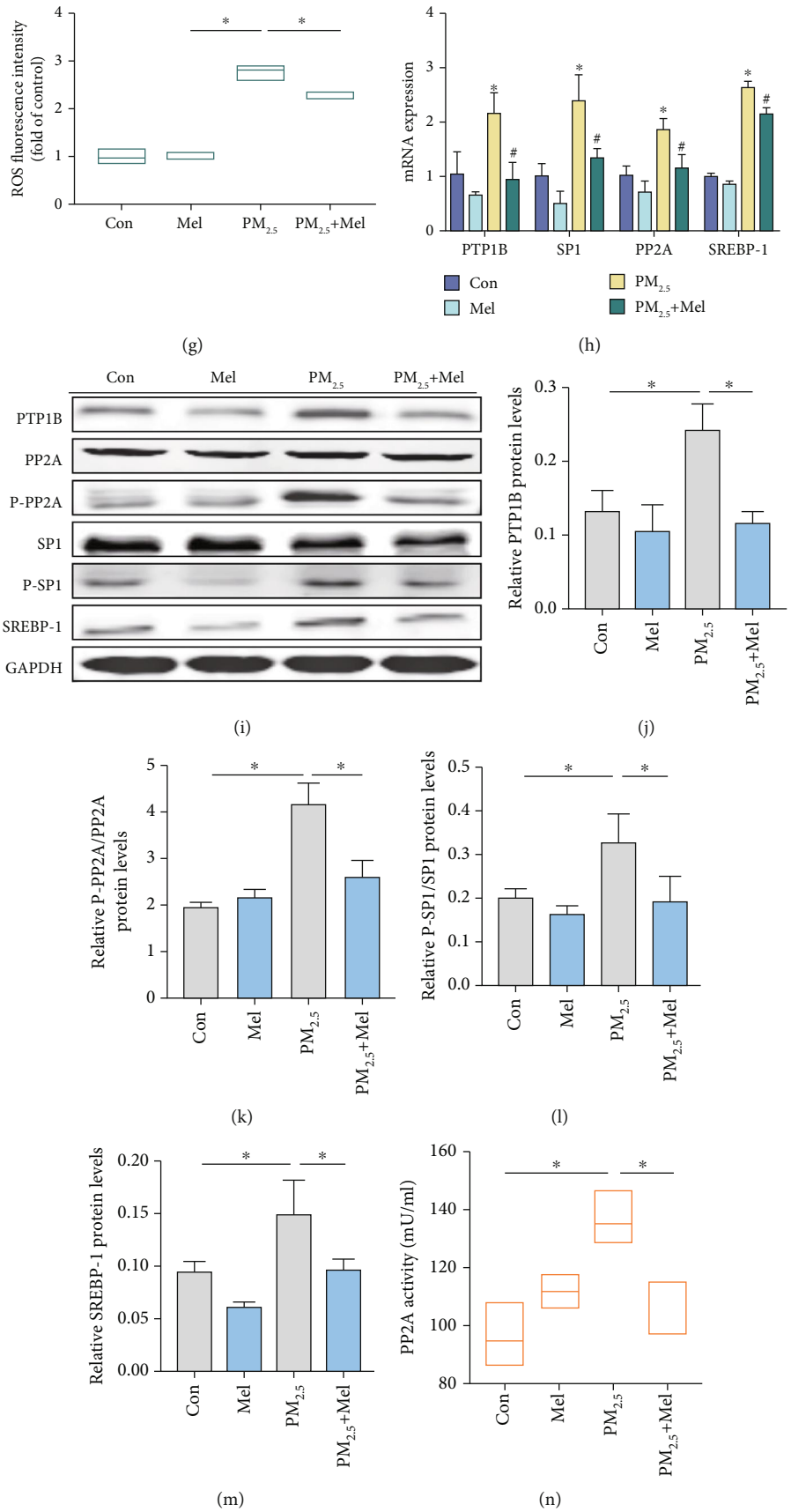

Figure 6: Continued.

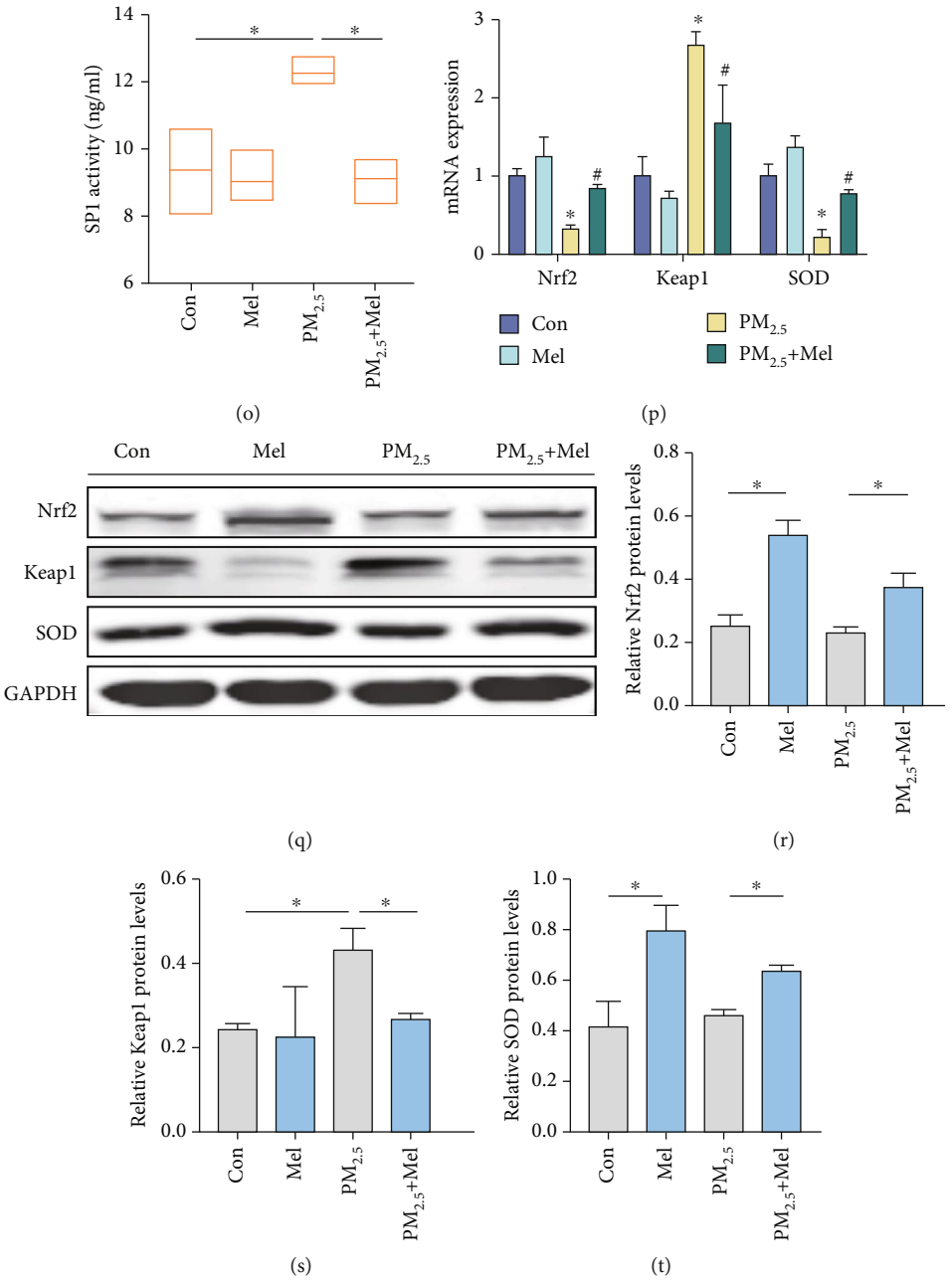

Figure 6: Melatonin alleviated $PM_{2.5}$-induced oxidative damage and upregulated PTP1B expression in vitro. (a) and (b) Cell ability. (c) Total cholesterol lipid levels (mmol/g). (d) Triacylglycerol lipid levels (mmol/g). (e) Representative confocal images of ROS. (f) Representative fluorescence intensity images obtained from flow cytometry in L02 cells. (g) Analysis of fluorescence intensity obtained from flow cytometry. (h) The mRNA expression of PTP1B, PP2A, SP1, and SREBP-1. (i) Western blotting of PTP1B, PP2A, P-PP2A, SP1, P-SP1, and SREBP-1. (j) Protein quantification of PTP1B. (k) Protein quantification of P-PP2A/PP2A. (l) Protein quantification of P-SP1/SP1. (m) Protein quantification of SREBP-1. (n) The activity of PP2A. (o) The activity of SP1. (p) The mRNA expression of Nrf2, Keap-1, and SOD. (q) Western blotting of Nrf2, Keap-1, and SOD. (r) Protein quantification of Nrf2. (s) Protein quantification of Keap-1. (t) Protein quantification of SOD. All values are presented as the mean ± SD. $^{*}P < 0.05$ for Con group vs $PM_{2.5}$ group and $^{\#}P < 0.05$ for $PM_{2.5}$ group vs $PM_{2.5}$+Mel group.

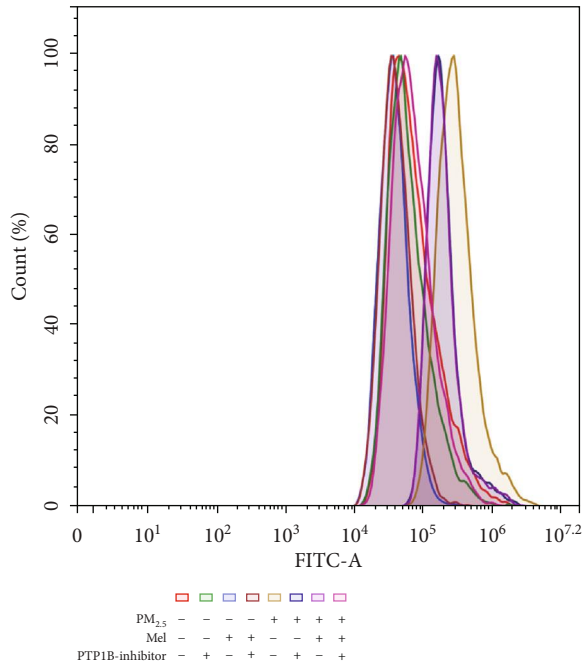

(a)

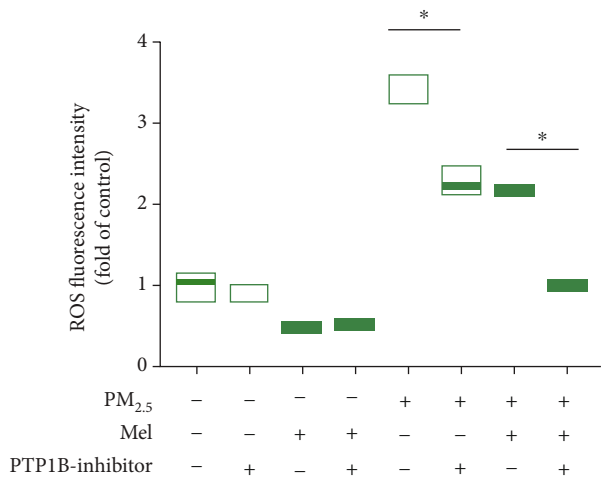

(b)

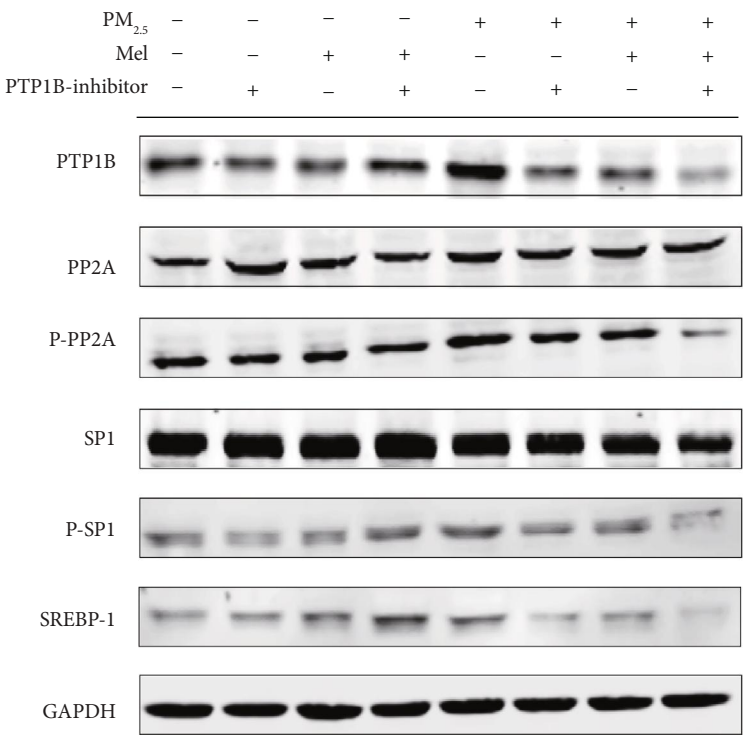

(c)

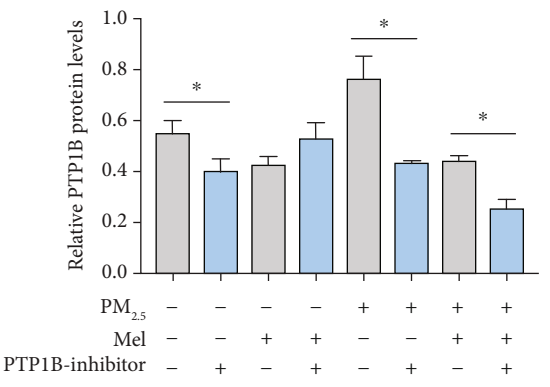

(d)

Figure 7: Continued.

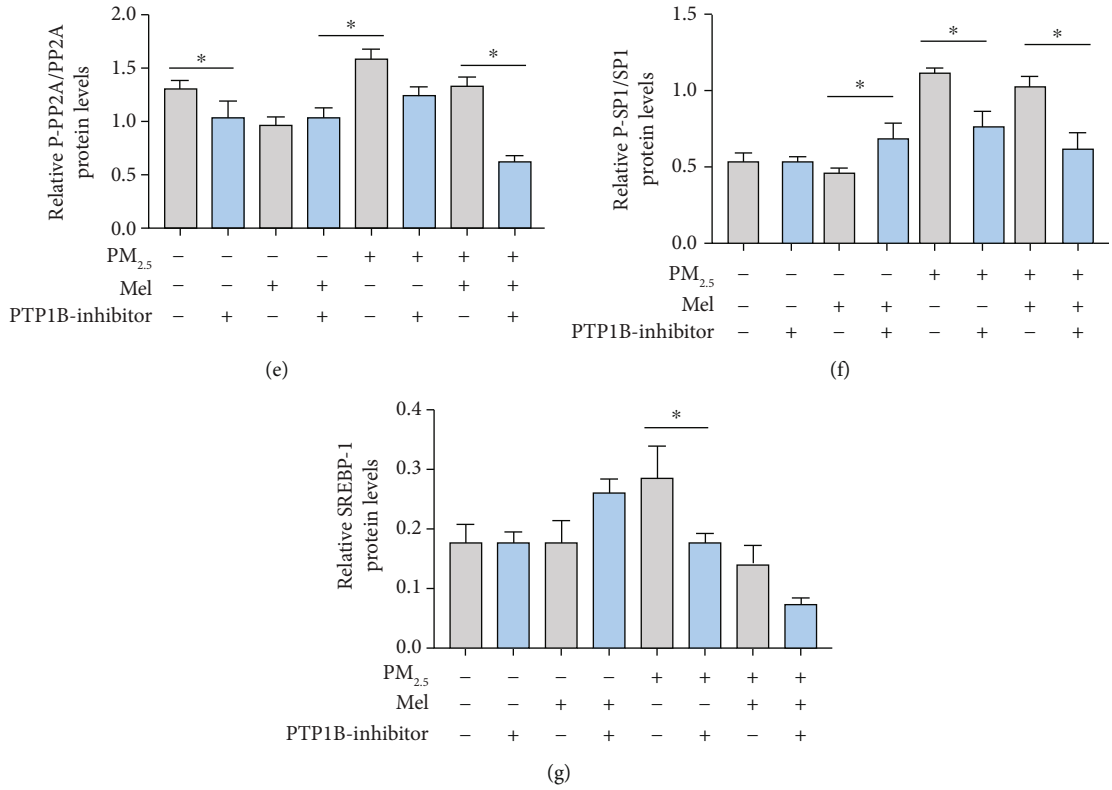

Figure 7: PTP1B inhibitor preconditioning eliminated lipid dysregulation in hepatocytes caused by $PM_{2.5}$ and melatonin intervention. (a) Representative fluorescence intensity images obtained from flow cytometry in L02 cells. (b) Analysis of fluorescence intensity obtained from flow cytometry. (c) Western blotting of PTP1B, PP2A, P-PP2A, SP1, P-SP1, and SREBP-1. (d) Protein quantification of PTP1B. (e) Protein quantification of P-PP2A/PP2A. (f) Protein quantification of P-SP1/SP1. (g) Protein quantification of SREBP-1. All values are presented as the mean ± SD. $^*P < 0.05$.

equal variance were tested by one-way ANOVA or two-way ANOVA. Among them, the data with only one variable of $PM_{2.5}$ adopted one-way ANOVA, and the data with two variables of melatonin and $PM_{2.5}$ adopted two-way ANOVA. The Kruskal-Wallis test was used for nonparametric data. A value of $p < 0.05$ indicates statistical significance. Each experiment was repeated at least three times.

3. Results

3.1. Melatonin Alleviated the $PM_{2.5}$-Induced Fatty Increase and Steatosis in $ApoE^{-/-}$ Mice. To evaluate the effects of $PM_{2.5}$ on liver lipid accumulation in mice, we first confirmed that $PM_{2.5}$ induced liver changes by ultrasound examination. The contrast of liver-kidney echo is one of the obvious manifestations of a fatty liver. Compared to the control group, ultrasonography showed that the echo of the liver parenchyma was high and dense, and the contrast sign of the liver and kidney was positive in the $PM_{2.5}$ group, but this expression was relieved in the melatonin group (Figure 1(a)). The anterior-posterior diameter and left-right diameter of the liver can reflect changes in liver size. Although these two indicators did not change significantly between the $PM_{2.5}$ and control groups, there was a significant difference between the $PM_{2.5}$ and melatonin groups (Figure 1(e)). Concordant with this, analysis of the body weights, liver weights, and liver coefficient of the mice showed that the liver size of the PM2.5 group was significantly higher than that of the control group, and that melatonin had a slight alleviating effect on liver weight gain (Supplementary Figure S1E-1G). Histological examinations of the liver are presented in Figures 1(b)–1(d). Electron microscopy images showed large lipid droplets, and HE and Oil Red O staining revealed notably enlarged adipocytes, fatty degeneration, and specific lipid accumulation in $PM_{2.5}$-treated mice compared to the control group. However, treatment with melatonin visibly alleviated these alterations. Next, changes in lipid content in the liver were examined. The levels of total cholesterol (TC) and triacylglycerols (TAGs) in the livers increased in response to $PM_{2.5}$, while melatonin treatment significantly decreased lipid levels (Figures 1 (g)and 1(h)). In addition, the Masson staining and qPCR analysis results of inflammatory factors (IL-1, IL-6, and TNF-α) in liver tissue showed that $PM_{2.5}$ could cause liver injury, and melatonin had a mitigating effect (Supplementary Figure S1A-1D). Taken together, these results suggested that $PM_{2.5}$ exposure could induce hepatic lipid metabolism disorders and that melatonin treatment had a beneficial effect on the liver.

3.2. Protective Effects of Melatonin on $PM_{2.5}$-Induced Oxidative Damage in Liver. Multiple studies have shown

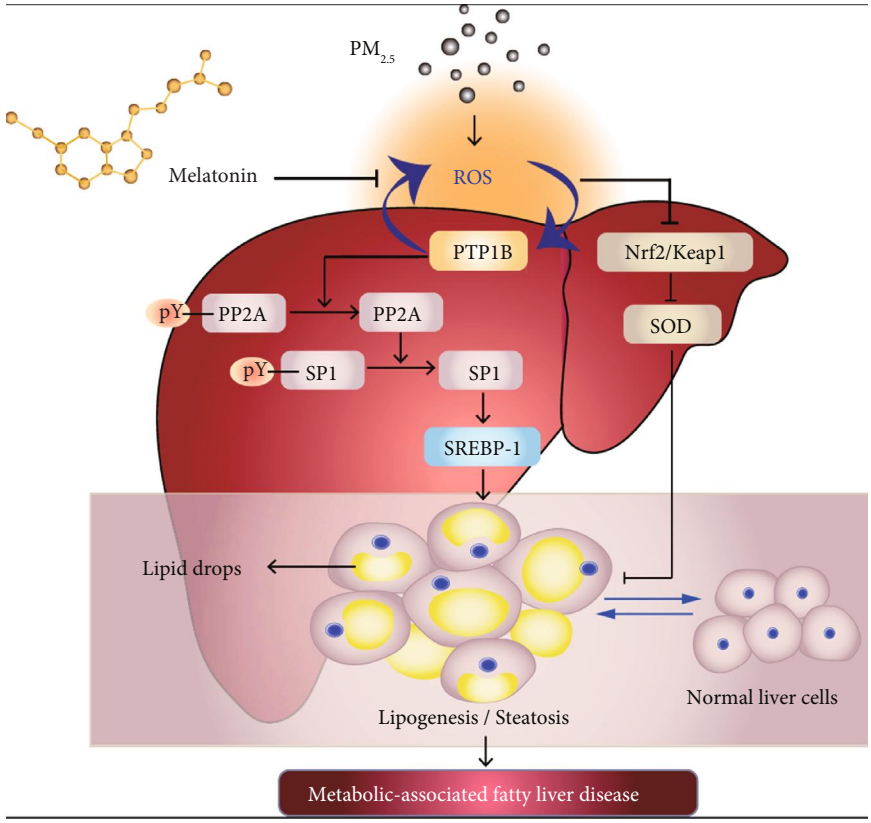

Figure 8: Schematic of melatonin ameliorating $PM_{2.5}$-induced hepatic lipid accumulation.

that $PM_{2.5}$ aggravates lipid metabolism disorder by inducing oxidative stress. To determine the effects of $PM_{2.5}$/melatonin on ROS production, liver sections were stained with the fluorescent probe DHE to evaluate ROS levels. As shown in the representative fluorescence micrographs (red fluorescence) and histogram of ROS relative fluorescence density (Figures 2(a) and 2(b)), $PM_{2.5}$ treatment increased ROS generation, while melatonin supplementation alleviated ROS generation. MDA and 4-HNE are important indexes of lipid peroxidation. According to the quantitative analysis, exposure to $PM_{2.5}$ resulted in significantly increased levels of MDA and 4-HNE, whereas melatonin treatment reversed these effects (Figures 2(c) and 2(d)). Moreover, the degree of oxidative stress was detected by examination of GSH-Px and SOD. As anticipated, $PM_{2.5}$ treatment reduced the activity of GSH-Px and SOD in the liver compared to the control. However, these two indicators were reversed by melatonin (Figures 2(e) and 2(f)). Subsequent analysis of the protein and mRNA expression levels of known indicators of oxidative stress, including Keap1, Nrf2, and SOD, was performed. In the present study, $PM_{2.5}$ exposure decreased Nrf2 and SOD mRNA expression and increased Keap1 mRNA expression, and these negative effects were mitigated by melatonin (Figure 2(g)). Consistently, compared with the control group, the expression of Nrf2/Keap1 and the SOD protein in the $PM_{2.5}$ group was not significantly different, but there were significant changes after melatonin treatment (Figures 2(h)–2(k)). However, this result did not rule out an impact on their gene expression. Overall, these data suggested that the antioxidative stress effects of melatonin might protect the liver from $PM_{2.5}$ exposure.

3.3. Melatonin Ameliorated Abnormal Liver Lipid Metabolism and Caused Elevated PTP1B Expression Induced by $PM_{2.5}$. To identify the potential mechanisms by which $PM_{2.5}$ or melatonin induced gene expression in lipid accumulation, qPCR analysis of genes related to lipid metabolism was examined in liver samples. Analysis of the mRNA expression levels showed that $PM_{2.5}$ exposure was associated with lipid metabolism disorder, and PTP1B, which is closely related to MAFLD, was an important upregulated transcription factor (Supplementary Figure S2). PTP1B is a key regulator of the antioxidant system and an activator of liver adipogenesis. Next, the regulation of downstream PTP1B on genes related to liver lipid metabolism was verified by qPCR analysis. As expected, $PM_{2.5}$ exposure significantly increased the expression of lipid accumulation markers (PP2A, SP1, and SREBP-1), whereas exogenous melatonin treatment decreased their levels (Figure 3(a)). Lipid accumulation plays an important role in the progression of MAFLD. Additionally, for further verification, Western blotting was carried out. $PM_{2.5}$ administration led to an increase in the accumulation of PTP1B, P-PP2A/PP2A, P-SP1/SP1, and SREBP-1, and subsequent analysis showed that melatonin inhibited their expression (Figures 3(b)–3(f)). However, the enzymatic activities of PP2A and SP1 did not change significantly in $PM_{2.5}$-exposed mice (Figures 3(g) and 3(h)). These results

could be greatly downregulated by melatonin treatment. All of the above data indicated that melatonin supplementation reduced adiposity accumulation triggered by $PM_{2.5}$.

3.4. $PM_{2.5}$ Exposure Caused Lipid Accumulation in L02 Cells by Inducing ROS Production. The cytotoxic effects of $PM_{2.5}$ on L02 cell viability was assessed by CCK-8 assay. As evidenced in Figure 4(a), the viability of L02 cells decreased with increasing doses of $PM_{2.5}$. Treatment with between 25 and 100 μg/mL $PM_{2.5}$ for 24 h showed significant differences compared with untreated cells. To detect the effects of $PM_{2.5}$ on lipid synthesis, L02 cells were exposed to various doses of $PM_{2.5}$ (0–100 μg/mL) for 24 h. As expected, the contents of T-CHO and TAGs in L02 cells gradually increased as the concentration of $PM_{2.5}$ increased (Figures 4(b) and 4(c)). Next, ROS generated by $PM_{2.5}$ treatment were detected by flow cytometry analysis quantification and confocal microscopy (Figures 4(d)–4(f)). Compared to the control group, the ROS fluorescence intensity was observably increased in $PM_{2.5}$-treated L02 cells, which occurred in a manner dependent on the $PM_{2.5}$ concentration. Then, activation of the PTP1B pathway was determined after $PM_{2.5}$ exposure. Quantitative measurements of protein expression showed that P-PP2A/PP2A, P-SP1/SP1, and SREBP-1 expression was dependent on the $PM_{2.5}$ concentration (Figures 4(g)–4(k)). In addition, activation of the Nrf2/Keap1 pathway was detected by Western blot. Low-dose $PM_{2.5}$ induced the upregulation of Nrf2 and SOD protein expression, while high-dose $PM_{2.5}$ inhibited their expression. The opposite trend was observed for Keap1 (Figures 4(l)–4(o)). Given the above data, although the effect indexes in the 25 μg/mL dose group were significantly different, the expression of the proteins in the PTP1B pathway was significantly different in the 50 μg/mL dose group, and the Nrf2/Keap1 pathway was inhibited in the 50 μg/mL dose group. For this reason, the concentration of $PM_{2.5}$ (50 μg/mL) was selected for subsequent experiments.

To obtain more details on the role of oxidative stress in $PM_{2.5}$-induced liver lipid accumulation, NAC (N-acetylcysteine) was added to L02 cells exposed to $PM_{2.5}$ (Figure 5). Representative images of BODIPY staining are shown in Figure 5(a). NAC treatment significantly abolished the $PM_{2.5}$-induced increase in lipid content in L02 cells. Flow cytometry and confocal microscopy data analysis indicated that the fluorescence intensity of the ROS generated in the NAC-treated cultures exposed to $PM_{2.5}$ (50 μg/mL) was significantly less than that in $PM_{2.5}$-exposed cells (Figures 5(b)–5(d)). Additionally, NAC treatment restored the expression of the proteins PTP1B, P-PP2A/PP2A, P-SP1/SP1, and SREBP-1 in $PM_{2.5}$-treated L02 cells to levels comparable with the control (Figures 5(e)–5(i)). $PM_{2.5}$ exposure initially triggered oxidative stress, which further led to lipid peroxidation. In short, the effects of $PM_{2.5}$ exposure on lipid accumulation in L02 cells were ROS dependent and involved PTP1B signalling.

3.5. Melatonin Alleviated $PM_{2.5}$-Induced Oxidative Damage and Lipid Accumulation In Vitro. To determine the dosage of melatonin to be used, CCK-8 assays were applied to examine cell viability. With increasing concentrations of melatonin, the viability of L02 cells first increased and then decreased, and 200 μmol/L melatonin showed a significant decrease compared to the control group (Figure 6(a)). Moreover, the effects of $PM_{2.5}$ and melatonin on cell viability were investigated (Figure 6(b)). Finally, 100 μmol/L melatonin was selected for further experiments. First, the protective effects of melatonin on lipid accumulation were detected by measuring the levels of TC and TAGs (Figures 6(c) and 6(d)). The results indicated that melatonin decreased the lipid levels in $PM_{2.5}$-induced L02 cells compared with $PM_{2.5}$ treatment alone. Flow cytometry and confocal microscopy data analysis indicated that treatment with melatonin could restore ROS to control levels (Figures 6(e)–6(g)). Furthermore, melatonin altered the mRNA levels of PTP1B, PP2A, SP1, and SREBP-1 in the presence of $PM_{2.5}$ (Figure 6(h)). Similarly, the levels of the proteins in the PTP1B pathway showed that melatonin reduced $PM_{2.5}$-induced lipid accumulation (Figures 6(i)–6(m)). Intriguingly, melatonin restored the $PM_{2.5}$-mediated increase in PP2A and SP1 activity to a normal level (Figures 6(n) and 6(o)). Moreover, $PM_{2.5}$ exposure decreased the Nrf2 and SOD mRNA expression and increased the Keap1 mRNA expression, and these negative effects were mitigated by melatonin (Figure 6(p)). Melatonin activation of the Nrf2/Keap1 pathway represented relief of oxidative stress after $PM_{2.5}$ treatment. Compared to the control group, Nrf2/Keap1 and SOD protein expression was significantly affected in the melatonin group but only slightly changed after $PM_{2.5}$ exposure (Figures 6(q)–6(t)). It could therefore be concluded that the relief of oxidative stress after melatonin treatment could alleviate fat accumulation in L02 liver cells.

3.6. Melatonin Regulated Hepatic Lipid Metabolism through the PTP1B and Nrf2 Signalling Pathways in $PM_{2.5}$-Treated L02 Cells. To confirm that $PM_{2.5}$-induced hepatocyte steatosis occurred through the upregulation of PTP1B, a specific inhibitor of PTP1B (10 μg/mL) was used in this study. Firstly, the dose was determined by PCR to detect the inhibitory effect on PTP1B mRNA expression (Supplementary Figure S3). As shown in Figures 7(a) and 7(b), both melatonin and the PTP1B inhibitor had significant ROS scavenging ability. Compared with $PM_{2.5}$ treatment alone, melatonin treatment decreased the ROS levels by approximately 40%, and the PTP1B inhibitor decreased the ROS levels by approximately 80%. The levels of melatonin and PTP1B inhibitor in $PM_{2.5}$-exposed cells were also significantly lower than those in the group treated with both melatonin and $PM_{2.5}$. Similar to melatonin, the inhibitor downregulated the expression of PTP1B and its downstream molecular proteins (PTP1B, P-PP2A/PP2A, P-SP1/SP1, and SREBP-1) that regulate lipid production. The synergistic effects of melatonin and the inhibitor were greater than the effects of melatonin alone (Figures 7(c)–7(g)). Consistent with the results above, PTP1B was the direct target gene of $PM_{2.5}$-induced oxidative stress, and inhibition of PTP1B expression downregulated the expression of its downstream gene SREBP-1 and reduced ROS production, thus reducing lipid production in L02 cells.

4. Discussion

Environmental $PM_{2.5}$ has been recognized as the largest global threat affecting human health, including the development of MAFLD [4]. The pathogenesis and molecular mechanisms of $PM_{2.5}$-induced MAFLD have not yet been well elucidated. In this study, we found that $PM_{2.5}$ induced oxidative stress, which activated PTP1B and in turn regulated ROS release with positive feedback. Moreover, melatonin alleviated the interference of liver fat metabolism disorder caused by $PM_{2.5}$ through regulation of the ROS-mediated PTP1B and Nrf2 signalling pathways.

MAFLD is a redefinition of NAFLD (nonalcoholic fatty liver disease). MAFLD represents a general overview of common liver metabolic disorders (not just nonalcoholics) and has multiple dominant drivers of subphenotypic response diseases. It covers more than NAFLD and has more specific diagnostic criteria [41]. Therefore, the more accurate and clear terminology of MAFLD was adopted in this work, which may provide a much wider applicability for our subsequent study to explore the toxic mechanism of $PM_{2.5}$. In our study, ultrasonography showed that in the $PM_{2.5}$ exposure group, the liver had a smooth contour, sharp edges, and increased parenchymal echo density, and positive contrast signs were also observed in the liver and kidney (Figure 1). The hepatorenal index is an important indicator of a fatty liver [42]. Similarly, the histopathological observation results (Oil Red O and HE staining) showed obvious fat vacuoles of varying sizes in the livers of $PM_{2.5}$-treated mice, which presented with severe steatosis (Figure 1). Exposure to $PM_{2.5}$ has been reported to cause systemic IR and increase the accumulation of hepatic lipids in the liver, which is consistent with our findings [43]. In addition, we observed increases in T-CHO and TAGs in mouse livers and human hepatocytes exposed to $PM_{2.5}$, indicating that the induced lipid metabolism disorders were severe, as evidenced by the lipid index (Figures 1 and 4). The liver is a central organ for lipid homeostasis and energy metabolism [44]. Liver steatosis is caused by an imbalance in lipid homeostasis, where lipid absorption or de novo fat production exceeds lipid oxidation or output [45]. Here, our results revealed that $PM_{2.5}$ exposure induced significant lipid accumulation in the liver accompanied by an increase in liver volume, suggesting that $PM_{2.5}$ exposure triggered pathological changes in liver morphology and function.

To date, many studies have demonstrated that MAFLD is closely related to oxidative stress induced by $PM_{2.5}$ exposure [5]. Oxidative stress is caused by the imbalance between the production of ROS and the ROS scavenging activity [46]. Excessive ROS results in increased adipogenesis and decreased β-oxidation of fatty acids, which leads to the accumulation of triacylglycerols in hepatocytes [47]. We studied the induction of ROS generation by $PM_{2.5}$ in $ApoE^{-/-}$ mice, and the data revealed that $PM_{2.5}$ promoted ROS production, decreased SOD activity, and induced lipid peroxidation (as evidenced by the levels of 4-HNE and MDA) (Figure 2). Consistent with the results of the animal experiments, $PM_{2.5}$ increased intracellular ROS in a dose-dependent manner in L02 cells (Figure 4). Compared with reliable evidence that $PM_{2.5}$ exposure can upregulate ROS pathways, the regulation and defence of antioxidant mechanisms are relatively scarce. We further examined the mRNA and protein levels of antioxidant stress markers, namely, Nrf2/Keap1 and SOD. The qPCR results showed that $PM_{2.5}$ acted by upregulating the Nrf2 inhibitor Keap1. Compared with the control group, Nrf2 protein expression was slightly downregulated in the $PM_{2.5}$ group, but there was no significant difference (Figure 2). The reason for this result may be that at the transcriptional and translational levels, the course of mRNA translation into proteins is adjusted by a variety of factors, which may lead to an inconsistency between mRNA and protein expression [48]. Interestingly, the expression of Nrf2 was upregulated in the low-dose $PM_{2.5}$ group and downregulated in the high-dose $PM_{2.5}$ group, while the expression of Keap1 showed the opposite trend (Figure 4). It may be that the low dose of $PM_{2.5}$ induces the body's stress response and activates Nrf2. However, with increasing exposure dose, $PM_{2.5}$ inhibits the Nrf2 pathway. Similarly, it has been found that low concentrations of $PM_{2.5}$ slightly upregulate Nrf2 expression, and subsequently, $PM_{2.5}$ treatment dose-dependently decreases Nrf2 expression [10]. These studies have shown that $PM_{2.5}$ induces ROS production and changes in antioxidant genes, which play vital regulatory roles in the progression of MAFLD.

ROS overproduction can modulate many cellular events involved in hepatic lipid metabolism diseases by regulating a variety of disease-related targets, such as PTP1B [49]. In addition, PTP1B levels were significantly elevated in the hepatocytes of fructose-fed hamsters, HFD-fed mice, and fatty liver and insulin-resistant animal models [50]. The overexpression of PTP1B in liver cells increased the expression level and transcriptional activity of SREBP1, which resulted in the increased synthesis of liver triacylglycerols and fatty acids [51]. This was due to the enhanced transcriptional activity of the recombinant SP1 site in the SREBP1 promoter by increasing the activity of PP2A when PTP1B was overexpressed [52]. This study found that $PM_{2.5}$ could upregulate PTP1B expression by inducing ROS generation, and the expression level of PTP1B and ROS production was dose-dependent (Figures 3, 4, and 6). Especially, $PM_{2.5}$ and melatonin did not affect the activity of PP2A and SP1 (Figure 3). This may be related to the posttranslational modification of proteins [53, 54]. NAC preconditioning inhibited $PM_{2.5}$-induced PTP1B overexpression, suggesting that ROS plays an important role in PTP1B activation after $PM_{2.5}$ exposure (Figure 5). Surprisingly, we found that PTP1B regulated by $PM_{2.5}$ had positive feedback regulation on ROS release. As shown in Figure 7, pretreatment of L02 cells with PTP1B inhibitors significantly reduced ROS production and subsequently downregulated the PTP1B downstream proteins PP2A, SP1, and SREBP1. Based on previous evidence, PTP1B KO mice showed decreased ROS production and lipid peroxidation in the liver [55]. To our knowledge, our results provide new evidence of the mechanism by which $PM_{2.5}$ exposure promotes the occurrence and development of MAFLD, demonstrating that $PM_{2.5}$ exposure activates the ROS/PTP1B pathway and that PTP1B regulates ROS by positive feedback.

Many studies have shown that the nocturnal indole melatonin produced by the pineal gland is effective against metabolic syndrome [56]. More recently, melatonin has been shown to reverse the harmful effects of fructose in the diet, and this animal model modulates metabolic pathways such as lipid production, β-oxidation, lipolysis, and gluconeogenesis [57]. Melatonin may also be ingested in the liver in a dose-dependent manner through specific cellular and nuclear receptors [58]. The pathogenesis of MAFLD is complex, but melatonin may be the key to the treatment of MAFLD. Furthermore, melatonin alleviated hepatic steatosis and lipid accumulation in ApoE$^{-/-}$ mice under different experimental conditions [59]. A previous animal study showed that ROS mediated lipopolysaccharide-induced SREBP-1c activation and lipid accumulation in the liver. Melatonin might be used as a pharmacological agent to prevent endotoxin-induced MAFLD [60]. Liver lipotoxicity is closely related to hepatic metabolic disorders caused by impaired fatty acid oxidation and increased ROS production [61]. It may be helpful to study the protective effects of melatonin on $PM_{2.5}$-induced hepatic fatty degeneration. Therefore, more research is encouraged to explore this issue. In our study, as expected, melatonin mitigated steatosis and decreased the lipid content of the liver during $PM_{2.5}$ damage. Both animal and cell experiments showed that melatonin effectively reduced ROS levels and helped to downregulate PTP1B and increase Nrf2 expression in $PM_{2.5}$-treated groups, thereby changing the effects of $PM_{2.5}$ exposure on liver lipid accumulation.

The schematic diagram summarizing these results and mechanisms shows that $PM_{2.5}$-induced ROS accumulation simultaneously promotes fat generation signal transduction by activating the PTP1B-PP2A-SP1-SREBP1 axis and inhibiting the Nrf2/Keap1-SOD axis, resulting in lipid accumulation and promotion of the occurrence and development of MAFLD. Moreover, melatonin plays an antioxidative stress role and regulates the ROS-mediated PTP1B and Nrf2 signalling pathways by inhibiting ROS production to alleviate the harmful effects induced by $PM_{2.5}$ (Figure 8). A comprehensive study of ROS targets could not only provide insight into the mechanism of $PM_{2.5}$-induced MAFLD but also give more evidence for the clinical applications of melatonin.

5. Conclusions

In summary, this study shows that $PM_{2.5}$ promoted the occurrence and development of MAFLD in ApoE$^{-/-}$ mice. Excess accumulation of $PM_{2.5}$-induced ROS could activate PTP1B, which in turn had a positive feedback regulation effect on ROS release. Our study is the first to show that melatonin alleviated the disturbance of $PM_{2.5}$-triggered hepatic steatosis and liver damage by regulating the ROS-mediated PTP1B and Nrf2 signalling pathways. These results suggest that melatonin administration may be a prospective therapy for the prevention and treatment of MAFLD associated with air pollution.

Data Availability

Most of data and materials generated or analyzed during this study are included in this manuscript. Other data are available from the corresponding authors on reasonable request.

Ethical Approval

The animal experiment in this study was approved by the Animal Ethics Committee of Capital Medical University (Ethics No. AEEI-2016-076).

Consent

Not applicable.

Conflicts of Interest

The authors declare they have no conflict of interest.

Authors' Contributions

Zhiwei Sun and Junchao Duan conceived and designed the experiments. Zhou Du, Shuang Liang, Jingyi Zhang, and Qing Xu performed the experiments. Zhou Du, Yang Li, Yang Yu, and Qing Xu analyzed the data. Zhiwei Sun and Junchao Duan contributed reagents/materials/analysis tools. Zhou Du and Junchao Duan wrote the paper.

Acknowledgments

This work was supported by the National Natural Science Foundation of China (91943301, 92043301, 81930091, and 81973077), Beijing Natural Science Foundation Program and Scientific Research Key Program of Beijing Municipal Commission of Education (KZ202110025040).

Supplementary Materials

Figure S1: liver damage effects of $PM_{2.5}$. Figure S2: mRNA expression levels associated with $PM_{2.5}$ exposure to liver injury. Figure S3: mRNA expression of PTP1B after treatment with PTP1B inhibitor. Table S1: concentrations of inorganic elements in $PM_{2.5}$. Table S2: content of water soluble ions in $PM_{2.5}$. Table S3: introduction of genes related to liver injury caused by $PM_{2.5}$. *(Supplementary Materials)*

References

[1] H. Wang, X. Shen, J. Liu et al., "The effect of exposure time and concentration of airborne $PM_{2.5}$ on lung injury in mice: a transcriptome analysis," *Redox biology*, vol. 26, article 101264, 2019.

[2] M.-X. Xu, C.-X. Ge, Y.-T. Qin et al., "Prolonged $PM_{2.5}$ exposure elevates risk of oxidative stress-driven nonalcoholic fatty liver disease by triggering increase of dyslipidemia," *Free Radical Biology and Medicine*, vol. 130, pp. 542–556, 2019.

[3] T. Li, R. Hu, Z. Chen et al., "Fine particulate matter ($PM_{2.5}$): the culprit for chronic lung diseases in China," *Chronic diseases and translational medicine*, vol. 4, no. 3, pp. 176–186, 2018.

[4] D. Li, Y. Li, G. Li, Y. Zhang, J. Li, and H. Chen, "Fluorescent reconstitution on deposition of $PM_{2.5}$ in lung and extrapulmonary organs," *Proceedings of the National Academy of Sciences of the United States of America*, vol. 116, no. 7, pp. 2488–2493, 2019.

[5] T. Jian, X. Ding, Y. Wu et al., "Hepatoprotective effect of loquat leaf flavonoids in $PM_{2.5}$-induced non-alcoholic fatty liver disease via regulation of IRs-1/Akt and CYP2E1/JNK pathways," *International journal of molecular sciences*, vol. 19, no. 10, p. 3005, 2018.

[6] S. Sun, Q. Yang, Q. Zhou et al., "Long-term exposure to fine particulate matter and non-alcoholic fatty liver disease: a prospective cohort study," *Gut*, vol. 71, no. 2, pp. 443–445, 2022.

[7] S. Spahis, E. Delvin, J. M. Borys, and E. Levy, "Oxidative stress as a critical factor in nonalcoholic fatty liver disease pathogenesis," *Antioxidants & redox signaling*, vol. 26, no. 10, pp. 519–541, 2017.

[8] S. Ding, C. Yuan, B. Si et al., "Combined effects of ambient particulate matter exposure and a high-fat diet on oxidative stress and steatohepatitis in mice," *PLoS One*, vol. 14, no. 3, article e0214680, 2019.

[9] F. Bessone, M. V. Razori, and M. G. Roma, "Molecular pathways of nonalcoholic fatty liver disease development and progression," *Cellular and molecular life sciences : CMLS*, vol. 76, no. 1, pp. 99–128, 2019.

[10] C. Ge, J. Tan, S. Zhong et al., "Nrf2 mitigates prolonged $PM_{2.5}$ exposure-triggered liver inflammation by positively regulating SIKE activity: protection by Juglanin," *Redox biology*, vol. 36, article 101645, 2020.

[11] J. P. Ribeiro, A. C. Kalb, P. P. Campos et al., "Toxicological effects of particulate matter ($PM_{2.5}$) on rats: bioaccumulation, antioxidant alterations, lipid damage, and ABC transporter activity," *Chemosphere*, vol. 163, pp. 569–577, 2016.

[12] M. J. Piao, M. J. Ahn, K. A. Kang et al., "Particulate matter 2.5 damages skin cells by inducing oxidative stress, subcellular organelle dysfunction, and apoptosis," *Archives of Toxicology*, vol. 92, no. 6, pp. 2077–2091, 2018.

[13] L. Chen, X. Zhang, L. Zhang, and D. Zheng, "Effect of saxagliptin, a dipeptidyl peptidase 4 inhibitor, on non-alcoholic fatty liver disease," *Diabetes, metabolic syndrome and obesity : targets and therapy*, vol. 13, pp. 3507–3518, 2020.

[14] A. Vivero, M. Ruz, M. Rivera et al., "Zinc supplementation and strength exercise in rats with type 2 diabetes: Akt and PTP1B phosphorylation in nonalcoholic fatty liver," *Biological trace element research.*, vol. 199, no. 6, pp. 2215–2224, 2021.

[15] Á. González-Rodríguez, M. P. Valdecantos, P. Rada et al., "Dual role of protein tyrosine phosphatase 1B in the progression and reversion of non-alcoholic steatohepatitis," *Molecular metabolism*, vol. 7, pp. 132–146, 2018.

[16] N. Aberdein, R. J. Dambrino, J. M. do Carmo et al., "Role of PTP1B in POMC neurons during chronic high-fat diet: sex differences in regulation of liver lipids and glucose tolerance," *American Journal of Physiology-Regulatory, Integrative and Comparative Physiology*, vol. 314, no. 3, pp. R478–R488, 2018.

[17] J. Zhou, K. Huang, and X. G. Lei, "Selenium and diabetes–Evidence from animal studies," *Free radical biology & medicine*, vol. 65, pp. 1548–1556, 2013.

[18] S. F. Bhat, S. E. Pinney, K. M. Kennedy et al., "Exposure to high fructose corn syrup during adolescence in the mouse alters hepatic metabolism and the microbiome in a sex-specific manner," *The Journal of physiology*, vol. 599, no. 5, pp. 1487–1511, 2021.

[19] B. Bilska, F. Schedel, A. Piotrowska et al., "Mitochondrial function is controlled by melatonin and its metabolites in vitro in human melanoma cells," *Journal of Pineal Research*, vol. 70, no. 3, p. e12728, 2021.

[20] K. H. Jung, S. W. Hong, H. M. Zheng et al., "Melatonin ameliorates cerulein-induced pancreatitis by the modulation of nuclear erythroid 2-related factor 2 and nuclear factor-kappaB in rats," *Journal of Pineal Research*, vol. 48, no. 3, pp. 239–250, 2010.

[21] J. I. Heo, D. W. Yoon, J. H. Yu et al., "Melatonin improves insulin resistance and hepatic steatosis through attenuation of alpha-2-HS-glycoprotein," *Journal of Pineal Research*, vol. 65, no. 2, article e12493, 2018.

[22] A. Stacchiotti, I. Grossi, R. García-Gómez et al., "Melatonin effects on non-alcoholic fatty liver disease are related to microRNA-34a-5p/Sirt1 axis and autophagy," *Cell*, vol. 8, no. 9, p. 1053, 2019.

[23] S. Bose, G. B. Diette, H. Woo et al., "Vitamin D status modifies the response to indoor particulate matter in obese urban children with asthma," *The journal of allergy and clinical immunology In practice*, vol. 7, no. 6, pp. 1815–1822.e2, 2019.

[24] K. D. Lu, P. N. Breysse, G. B. Diette et al., "Being overweight increases susceptibility to indoor pollutants among urban children with asthma," *The Journal of allergy and clinical immunology*, vol. 131, no. 4, pp. 1017–1023, 2013.

[25] O. Jamialahmadi, R. M. Mancina, E. Ciociola et al., "Exome-wide association study on alanine aminotransferase identifies sequence variants in the GPAM and APOE_associated with fatty liver disease," *Gastroenterology*, vol. 160, no. 5, pp. 1634–1646.e7, 2021.

[26] N. D. Palmer, B. Kahali, A. Kuppa et al., "Allele specific variation at *APOE* increases non-alcoholic fatty liver disease and obesity but decreases risk of Alzheimer's disease and myocardial infarction," *Human molecular genetics*, vol. 30, no. 15, pp. 1443–1456, 2021.

[27] W. C. Huang, J. W. Xu, S. Li, X. E. Ng, and Y. T. Tung, "Effects of exercise on high-fat diet-induced non-alcoholic fatty liver disease and lipid metabolism in ApoE knockout mice," *Nutrition & metabolism*, vol. 19, no. 1, p. 10, 2022.

[28] J. H. Dumolt, M. S. Patel, and T. C. Rideout, "Gestational hypercholesterolemia programs hepatic steatosis in a sex-specific manner in ApoE-deficient mice," *The Journal of nutritional biochemistry*, vol. 101, article 108945, 2022.

[29] S. Liu, R. Weng, X. Gu, L. Li, and Z. Zhong, "Association between apolipoprotein E gene polymorphism and nonalcoholic fatty liver disease in Southern China: a case-control study," *Journal of clinical laboratory analysis*, vol. 35, no. 12, article e24061, 2021.

[30] J. Xu, Y. Guo, X. Huang et al., "Effects of DHA dietary intervention on hepatic lipid metabolism in apolipoprotein E-deficient and C57BL/6J wild-type mice," *Biomedicine & pharmacotherapy = Biomedecine & pharmacotherapie*, vol. 144, article 112329, 2021.

[31] Y. Q. Hua, Y. Zeng, J. Xu, and X. L. Xu, "Naringenin alleviates nonalcoholic steatohepatitis in middle-aged $Apoe^{-/-}$mice: role of SIRT1," *Phytomedicine : international journal of phytotherapy and phytopharmacology*, vol. 81, article 153412, 2021.

[32] A. Stachowicz, A. Wiśniewska, K. Kuś et al., "Diminazene aceturate stabilizes atherosclerotic plaque and attenuates

hepatic steatosis in apoE-knockout mice by influencing macrophages polarization and taurine biosynthesis," *International journal of molecular sciences*, vol. 22, no. 11, p. 5861, 2021.

[33] Y. Zhang, H. Hu, Y. Shi et al., "^{1}H NMR-based metabolomics study on repeat dose toxicity of fine particulate matter in rats after intratracheal instillation," *The Science of the total environment*, vol. 589, pp. 212–221, 2017.

[34] J. Liu, S. Liang, Z. Du et al., "$PM_{2.5}$ aggravates the lipid accumulation, mitochondrial damage and apoptosis in macrophage foam cells," *Environmental Pollution*, vol. 249, pp. 482–490, 2019.

[35] M. Zhang, J. Lin, S. Wang et al., "Melatonin protects against diabetic cardiomyopathy through Mst1/Sirt3 signaling," *Journal of Pineal Research*, vol. 63, no. 2, p. e12418, 2017.

[36] J. Hu, L. Zhang, Y. Yang et al., "Melatonin alleviates postinfarction cardiac remodeling and dysfunction by inhibiting Mst1," *Journal of Pineal Research*, vol. 62, no. 1, p. e12368, 2017.

[37] WHO, "Air Quality Guidelines: Global Update 2005," in *Particulate Matter, Ozone, Nitrogen Dioxide and Sulfur Dioxide*, World Health Organization, Geneva, Switzerland, 2005.

[38] R. Ning, Y. Li, Z. Du et al., "The mitochondria-targeted antioxidant MitoQ attenuated $PM_{2.5}$-induced vascular fibrosis via regulating mitophagy," *Redox biology*, vol. 46, article 102113, 2021.

[39] Z. Zhang, S. Hu, P. Fan et al., "The roles of liver inflammation and the insulin signaling pathway in $PM_{2.5}$ instillation-induced insulin resistance in Wistar rats," *Disease markers*, vol. 2021, Article ID 2821673, 11 pages, 2021.

[40] M. Catta-Preta, L. S. Mendonca, J. Fraulob-Aquino, M. B. Aguila, and C. A. Mandarim-de-Lacerda, "A critical analysis of three quantitative methods of assessment of hepatic steatosis in liver biopsies," *Virchows Archiv : an international journal of pathology*, vol. 459, no. 5, pp. 477–485, 2011.

[41] M. Eslam, A. J. Sanyal, J. George et al., "MAFLD: a consensus-driven proposed nomenclature for metabolic associated fatty liver disease," *Gastroenterology*, vol. 158, no. 7, pp. 1999–2014.e1, 2020.

[42] P. Avramovski, M. Avramovska, Z. Nikleski, B. Ilkovska, K. Sotiroski, and E. Sikole, "The predictive value of the hepatorenal index for detection of impaired glucose metabolism in patients with non-alcoholic fatty liver disease," *Indian journal of gastroenterology : official journal of the Indian Society of Gastroenterology*, vol. 39, no. 1, pp. 50–59, 2020.

[43] C. Liu, X. Xu, Y. Bai et al., "Air pollution-mediated susceptibility to inflammation and insulin resistance: influence of CCR2 pathways in mice," *Environmental Health Perspectives*, vol. 122, no. 1, pp. 17–26, 2014.

[44] Z. Wu, H. Ma, L. Wang et al., "Tumor suppressor ZHX2 inhibits NAFLD-HCC progression via blocking LPL- mediated lipid uptake," *Cell death and differentiation*, vol. 27, no. 5, pp. 1693–1708, 2020.

[45] S. L. Friedman, B. A. Neuschwander-Tetri, M. Rinella, and A. J. Sanyal, "Mechanisms of NAFLD development and therapeutic strategies," *Nature Medicine*, vol. 24, no. 7, pp. 908–922, 2018.

[46] X. F. Hu, G. Xiang, T. J. Wang et al., "Impairment of type H vessels by NOX2-mediated endothelial oxidative stress: critical mechanisms and therapeutic targets for bone fragility in streptozotocin-induced type 1 diabetic mice," *Theranostics*, vol. 11, no. 8, pp. 3796–3812, 2021.

[47] A. Mansouri, C. H. Gattolliat, and T. Asselah, "Mitochondrial dysfunction and signaling in chronic liver diseases," *Gastroenterology*, vol. 155, no. 3, pp. 629–647, 2018.

[48] S. Lin, C. Cao, Y. Meng et al., "Comprehensive analysis of the value of RAB family genes in prognosis of breast invasive carcinoma," *Bioscience Reports*, vol. 40, no. 5, 2020.

[49] J. Dong, S. Viswanathan, E. Adami et al., "Hepatocyte-specific IL11 cis-signaling drives lipotoxicity and underlies the transition from NAFLD to NASH," *Nature Communications*, vol. 12, no. 1, p. 66, 2021.

[50] C. Proença, D. Ribeiro, M. Freitas, F. Carvalho, and E. Fernandes, "A comprehensive review on the antidiabetic activity of flavonoids targeting PTP1B and DPP-4: a structure-activity relationship analysis," *Critical reviews in food science and nutrition.*, vol. 62, no. 15, pp. 4095–4151, 2022.

[51] X. Zhou, L. L. Wang, W. J. Tang, and B. Tang, "Astragaloside IV inhibits protein tyrosine phosphatase 1B and improves insulin resistance in insulin-resistant HepG2 cells and triglyceride accumulation in oleic acid (OA)-treated HepG2 cells," *Journal of Ethnopharmacology*, vol. 268, article 113556, 2021.

[52] H. Wu, T. Zhang, F. Pan et al., "MicroRNA-206 prevents hepatosteatosis and hyperglycemia by facilitating insulin signaling and impairing lipogenesis," *Journal of Hepatology*, vol. 66, no. 4, pp. 816–824, 2017.

[53] N. Zheng and N. Shabek, "Ubiquitin ligases: structure, function, and regulation," *Annual Review of Biochemistry*, vol. 86, no. 1, pp. 129–157, 2017.

[54] T. Narita, B. T. Weinert, and C. Choudhary, "Functions and mechanisms of non-histone protein acetylation," *Nature reviews Molecular cell biology*, vol. 20, no. 3, pp. 156–174, 2019.

[55] M. F. Hsu, S. Koike, A. Mello, L. E. Nagy, and F. G. Haj, "Hepatic protein-tyrosine phosphatase 1B disruption and pharmacological inhibition attenuate ethanol-induced oxidative stress and ameliorate alcoholic liver disease in mice," *Redox biology*, vol. 36, article 101658, 2020.

[56] J. Yin, Y. Li, H. Han et al., "Melatonin reprogramming of gut microbiota improves lipid dysmetabolism in high-fat diet-fed mice," *Journal of Pineal Research*, vol. 65, no. 4, article e12524, 2018.

[57] F. J. Valenzuela-Melgarejo, C. Caro-Díaz, and G. Cabello-Guzmán, "Potential crosstalk between fructose and melatonin: a new role of melatonin—inhibiting the metabolic effects of fructose," *International journal of endocrinology*, vol. 2018, Article ID 7515767, 11 pages, 2018.

[58] C. Venegas, J. A. García, C. Doerrier et al., "Analysis of the daily changes of melatonin receptors in the rat liver," *Journal of Pineal Research*, vol. 54, no. 3, pp. 313–321, 2013.

[59] F. Bonomini, G. Favero, L. F. Rodella, M. H. Moghadasian, and R. Rezzani, "Melatonin modulation of Sirtuin-1 attenuates liver injury in a hypercholesterolemic mouse model," *BioMed Research International*, vol. 2018, Article ID 7968452, 9 pages, 2018.

[60] X. Chen, C. Zhang, M. Zhao et al., "Melatonin alleviates lipopolysaccharide-induced hepatic SREBP-1c activation and lipid accumulation in mice," *Journal of Pineal Research*, vol. 51, no. 4, pp. 416–425, 2011.

[61] B. Sun, J. Zhou, Y. Gao et al., "Fas-associated factor 1 promotes hepatic insulin resistance via JNK signaling pathway," *Oxidative medicine and cellular longevity*, vol. 2021, Article ID 3756925, 10 pages, 2021.